NASA TECHNICAL NOTE

NASA TN D-6763

EFFECT OF CASING BOUNDARY-LAYER REMOVAL ON NOISE OF A TURBOFAN ROTOR

by Arthur W. Goldstein, Frederick W. Glaser, and James W. Coats

Lewis Research Center
Cleveland, Ohio 44135

NATIONAL AERONAUTICS AND SPACE ADMINISTRATION • WASHINGTON, D. C. • APRIL 1972

1. Report No.	2. Government Accession No.	3. Recipient's Catalog No.
NASA TN D-6763		

4. Title and Subtitle
EFFECT OF CASING BOUNDARY-LAYER REMOVAL ON NOISE OF A TURBOFAN ROTOR

5. Report Date
April 1972

6. Performing Organization Code

7. Author(s)
Arthur W. Goldstein, Frederick W. Glaser, and James W. Coats

8. Performing Organization Report No.
E-6727

9. Performing Organization Name and Address
Lewis Research Center
National Aeronautics and Space Administration
Cleveland, Ohio 44135

10. Work Unit No.
132-80

11. Contract or Grant No.

12. Sponsoring Agency Name and Address
National Aeronautics and Space Administration
Washington, D.C. 20546

13. Type of Report and Period Covered
Technical Note

14. Sponsoring Agency Code

15. Supplementary Notes

16. Abstract

The effect of casing boundary-layer removal on noise produced by a turbofan rotor was measured. The outlet guide vanes were removed for these tests. A comparison was made between the noise measurements when the boundary layer was bled off and under zero bleed conditions. When the boundary layer was removed, overall sound pressure level was reduced 2 dB with moderate blade loading and 3 dB with heavier blade loading. An analysis of the changes in the spectral density with bleed is presented.

17. Key Words (Suggested by Author(s))	18. Distribution Statement
Noise; Fan; Rotor; Boundary layer bleed; Blade boundary layer interaction noise	Unclassified - unlimited

19. Security Classif. (of this report)	20. Security Classif. (of this page)	21. No. of Pages	22. Price*
Unclassified	Unclassified	39	$3.00

* For sale by the National Technical Information Service, Springfield, Virginia 22151

EFFECT OF CASING BOUNDARY-LAYER REMOVAL ON NOISE OF A TURBOFAN ROTOR

by Arthur W. Goldstein, Frederick W. Glaser, and James W. Coats

Lewis Research Center

SUMMARY

The effect of casing boundary-layer removal on noise produced by a turbofan rotor was measured. The outlet guide vanes were removed for these tests. A comparison was made between the noise measurements when the boundary layer was bled off and under zero bleed conditions. When the boundary layer was removed, overall sound pressure level was reduced 2 decibels with moderate blade loading and 3 decibels with heavier blade loading.

A small reduction in blade passing tone was obtained by boundary-layer bleed. In a complete subsonic fan stage, this effect might be expected to be larger, particularly for close axial spacing between the blade rows; for a complete stage with a transonic rotor, this reduction would be negligible because of the dominance of shock noises.

In broad band noise, a reduction of about 5 decibels was obtained in the low frequency region (about 150 to 250 Hz); this is associated with a change in the level of jet noise and also in the level of internal noise. A reduction was obtained in a broad band noise component located in the region of 2800 hertz. This noise component is also sensitive to loading and probably arises from the vortex shedding and turbulence which accompany separation of the flow from the blade surface in the region near the blade tips, because of the influence of the casing boundary layer. An additional broad band noise is produced at the blade tips as the turbulence causes fluctuations of the blade lift. This noise, which has a very broad range with a maximum in the low frequency end, is noticeably reduced by bleeding the boundary layer.

INTRODUCTION

The noise produced by high bypass turbofan engines has a number of sources such as the fan, the core compressor and turbine, the fan and engine jets, and the gears.

The fan is generally a major noise producer; its noise is greatly influenced by the rotor blade tips because of the high relative gas velocity. The conditions under which these blade tips operate can be significant. Tests were made to find the influence of the boundary layer at the fan casing on the noise produced by rotor blading; these tests were conducted by comparison of noise with and without boundary-layer bleed in a test engine without guide vanes.

The effect of such a boundary layer can cause noise in several ways:

(1) Turbulence in the free stream near the boundary layer (and generated by this layer) could cause fluctuations in the flow field near the rotor blade tips and, therefore, pressure fluctuations on the blade surfaces and noise production.

(2) Separation of flow from the blade tips can occur because of high angle of attack. In the casing boundary layer, the flow velocity is in the axial direction and assumes low values compared to those in the free stream. Since the inflow direction relative to the blading is then at a high angle of attack in the boundary layer, separation of the flow from the blading results. Separation is not limited to the region of the blade tip immersed in the casing boundary layer. The radially adjacent region of the span has low pressure regions which suck the dead air from the blade tips into the boundary layer flowing on nearby portions of the blade and thicken it. The thickened boundary layer on the blade surfaces exterior to but near the casing boundary layer promotes separation there. The spanwise extent to which flow separation is tripped off by the casing boundary layer depends heavily on the aerodynamic loading of the blading.

In a complete fan stage, the large wakes generated by the rotor blade tips pass over the stator vanes periodically causing them to radiate a tone at the blade passing frequency. Removal of the boundary layer upstream of the rotor may therefore be expected to reduce the noise from outlet guide vanes as well as noise from the turbulent flow reacting with the rotor blade tips.

The tests reported here provide information on the effect of the casing boundary layer on noise produced by the rotor only; the outlet guide vanes were removed for this set of engine tests. Since the engine support struts are well downstream of the rotor (about three blade chords), they are believed to be generating only a small tone at the blade passing frequency. The broad band noise generated thereby is not known, but it should be small at least in the front quadrant of the radiation field.

SYMBOLS

A area of acoustically radiating surface

a_o sonic speed in atmosphere

C_L fluctuation of airfoil lift coefficient

c	airfoil chord
f	frequency of sound
f_f	frequency of blade passing tone of fan
f_s	frequency of blade passing tone of supercharger
K_1, K_2, etc.	proportionality constants
k	reduced frequency, $-\omega c/2V$
L	wake thickness or characteristic length
N	integer, $N \geq 0$
p	gas pressure, acoustic pressure fluctuation
Q	dimensionless form of pressure spectral density
R	distance from source of sound
S	Strouhal number, fL/V
t	time
t_e	thickness of trailing edge of rotor blades
V	flow velocity of gas in boundary layer
V_β, V_α	component of flow velocity of gas
V_c	convection velocity, jet sources
V_o	free stream velocity, air
W	acoustic power radiated
w	turbulent upwash normal to free stream velocity
w_o	upwash amplitude in frequency range w to $w + dw$
w_α, w_β	components of turbulent velocity
X	blade pitch, in rotational direction
y	distance from wall
α	fluctuation of flow angle
β_2	angle of blade section camber line at trailing edge, relative to machine axis
δ	boundary-layer thickness
δ^*	boundary-layer displacement thickness
Δ	blade tip clearance

θ angular coordinate, engine field, measured from forward centerline

θ^* momentum thickness of boundary layer

ρ_o density of gas in atmosphere

φ Sears' function

ψ_w, ψ_p spectral densities of turbulence correlation, wall pressure

ω frequency, rad/sec

$\overline{\omega}$ rotor blade loss coefficient

Subscripts:

α, β running coordinate indexes (tenser notation)

APPARATUS

The engine tested was a high bypass turbofan engine manufactured by the Lycoming Division of the AVCO Corporation. A schematic section is shown in figure 1. The nominal cruise speed of the fan is 6440 rpm; the tests were conducted without outlet guide vanes at 5800 rpm to conserve engine life. The rotor has 40 blades of 10.16-centimeter (4-in.) chord; tip diameter is 0.978 meter (38.5 in.).

The acoustic tests of the unmodified engine are reported in reference 1. As previously, the inlet cowl was replaced by a static-engine-test bellmouth intake. The present tests required modification from the original version: the stators downstream of the fan rotor were removed, and the bleed system was installed (fig. 2). The double slot was used because it is more efficient than the single; less volume is required to remove the boundary layer, since it is removed before some diffusion into the free stream occurs. The slots in the casing can be seen in detail in figure 3. The boundary layer is bled from the fan casing before passing through the rotor. At the bleed site the pressure is lower than that in the atmosphere. An ejector was therefore required to pump this low energy air back into the atmosphere; it was activated by an air line supplying about a 2.7 kilogram per second (6 lbm/sec) flow at a 357 000 newton per square meter (45 psi) gage pressure. An overall view of the test site is shown in figure 4.

Small pressure rakes measured the boundary-layer thickness just upstream of the rotor (fig. 3). Microphones were placed on a 30.48-meter (100-ft) radius, 1.22 meters (4 ft) off the ground (same as engine axis) in aximuthal locations at 10^o intervals from 0^o (front) to 160^o. In later tests microphones were located only at 0^o, 30^o, 40^o, 50^o, 90^o, and 130^o in order to reduce the engine running time. Acoustic data were reduced on line using a 1/3-octave band width analyzer; they were also recorded on tape for

later processing in 64- and 16-hertz bandwidth analyses. The data shown here were uncorrected for line loss. This line correction schedule is as follows:

Frequency, kHz:	3.15	4	5	6.3	8	10	12.5	16	20
Corrections, dB:	1	1	1	1	2	3	5	6	7

The fan jet was annular and surrounded the central engine exhaust jet. Between the two jets, at the nozzle exit, there was a dead air space (see fig. 5); a central body inside the engine exhaust flow produced an additional space near the axis.

TEST CONDITIONS

The equivalent (corrected) operating speed of the engine at test conditions was 5800 rpm. The outlet guide vanes were removed, and the fan nozzle areas were 0.330 and 0.313 square meter (512 and 486 in.^{2}). The weight flow with the 0.330-square-meter nozzle was about the same as when the guide vanes were in; the rotor operating condition may therefore be taken as the same. Calculations based on survey data with the 0.330-square-meter nozzle supplied by Lycoming showed a blade tip relative Mach number of 0.94 when the blade tip speed was 297 meters per second (975 ft/sec). The relative inflow angle at the rotor blade tips was 67.1°, and the diffusion factor (a measure of the blade loading) was about 0.36, which is a moderate level. The fan stage was operating at maximum efficiency, so the rotor blades were probably at the high incidence angle end of the loss curve. With the 0.313-square-meter nozzle area, calculations showed the relative flow angle increased to 69° and the diffusion factor to 0.470. Profile losses were estimated to increase about 25 percent at the blade tips when the nozzle size was reduced.

Bleed rates were set at 0, 0.816, and 1.0 kilogram per second (0, 1.8, and 2.2 lb/sec). (These flow rates were 0, 1.2, and 1.4 percent of the fan airflow.) Larger rates were possible, but these rates were found to affect the potential flow outside the boundary layer.

When no boundary-layer bleed was used, a smooth spool-piece was used in front of the rotor to avoid disturbance due to the presence of the bleed slots. This procedure required that the noise data with bleed be obtained on different days than when the no bleed data were obtained.

All data were obtained when the wind velocity was 5.1 meters per second (10 knots) or less.

TEST RESULTS

Boundary Layer

The boundary-layer velocity profiles downstream of the second bleed slot and just upstream of the rotor are shown in figure 6. When there is no bleed, the boundary-layer velocity reaches 90 percent of the free-stream value at 7.6 millimeters (0.3 in.) from the casing. Thus, the blade tips are immersed in the boundary layer. The static tip clearance is 3.3 millimeters (0.13 in.) where the velocity ratio is only 0.55. (Since operation was at only 77 percent of the speed of mechanical design, it is believed the running clearance was not much different, although the actual value is not known.) The displacement thicknesses for various bleed rates are given in table I.

TABLE I. - DISPLACEMENT THICKNESS

FOR VARIOUS BLEED RATES

Bleed, percent of flow	Displacement thickness, mm	Distance for $V/V_0 = 0.9$, mm
0	3.6	7.6
1.2	1.2	4.1
1.4	.33	0

The distance at which $V = 0.9\ V_0$ is listed because at this velocity the angle of incidence on the blade tips has increased 2.3° over the value in the potential flow region. Although this represents a substantial increase in aerodynamic loading, it is not sufficient to cause breakdown of the flow over the blades. Thus, if the running clearance of the blades is 3.3 millimeters, the velocity ratio at the blade tip section is 0.53 with an increase of 10° in the angle of attack. This is too high for efficient operation. Separation at nonzero bleed rates may also be caused by end flow through the clearance space.

Noise Data

The effects of boundary-layer bleed are shown in several types of spectrograms. One-third-octave bandwidth data are shown in figures 7 and 8. A bandwidth of 64 hertz was used for the spectrograms of figures 9 and 10. Additional spectrograms are presented in the appendix. These spectrograms include more microphone locations, ex-

tended frequency range, and smaller bandwidth data. All these data were reduced from samples having 4-second durations on the tape recordings. The accuracy of the 1/3-octave spectrograms may be estimated from the oscilloscope tracings of 12 separate spectrograms of 4-second samples (fig. 11). Over most of the spectrum the extreme fluctuation is 2 decibels, but in the bands containing the blade passing tone (3870 Hz) and its harmonics (7740 and 11 600 Hz) the fluctuations are 3 to 5 decibels. For blade passing tones of greater accuracy, four 32-second samples were obtained, and some typical data are shown in figure 12. The extremes in these cases differ by less than 2 decibels; extreme deviation from the mean is about 1 decibel.

The spectrograms show noise reduction resulting from boundary-layer bleed depending on frequency region, direction of radiation, and fan nozzle size. Overall sound pressure levels are reduced 2 decibels by bleeding with the large fan nozzle, and the levels are reduced 3 decibels by bleeding with the small fan nozzle. Almost the entire reduction in noise takes place with a bleed rate of 1.2 percent. This rate is adequate to remove the boundary layer from the blade tips so that they operate at a favorable incidence angle.

Analysis of Noise Data

Discrete tones. - The spectrographs (see, e.g., fig. 13) show discrete tones which are blade passing tones for the fan and first-stage supercharger (40 blades) at 3900 hertz and the overtones at 7800, 11 700, 15 600 hertz. The blade tone for the second-stage supercharger shows up at 4680 hertz (48 blades), and its harmonics are at 9360 and 14 040 hertz. Figure 1 shows the supercharger blading to be compactly arranged, so interaction tones may be expected; these tones occur at 5460, 8600, 10 920, 12 490, 13 260, 16 390, and 17 160 hertz, and their frequency values f follow the relation

$$f = N(f_s - f_f) + f_f$$

(The tone at 7000 Hz and $N = 4$ does not appear.)

The discrete tone components shown in the spectra were not sufficiently steady to provide reliable amplitudes since these were only 4-second averages. Samples of 32-second duration were used to find the discrete tone amplitudes on the 1/3-octave spectrographs. Not all these data were useable, since in some cases the amplitude of the band containing the blade passing tone did not clearly stand out from the amplitude of

adjacent filter bands. The suitable noise level data are summarized in table II.

TABLE II. - NOISE LEVEL OF

BLADE PASSING TONE

Bleed, percent	Microphone location, deg			
	0	30	40	50
	Noise, dB			
None	92.5	93.5	95.5	99.0
1.4	90.5	93.5	93.5	97.5

The effect of bleed is seen to be small. The noise reduction would be much greater for a complete fan stage because the size of the wakes discharged from the rotor blade tips would be reduced when the casing boundary layer is bled off. Stator blade radiation of blade passing tone would be reduced with these smaller wakes. For supersonic rotors the noise reduction due to boundary-layer bleed should be less, because of the substantial blade passing tone generated by shocks on the leading edges of rotor blades.

Broad Band Noise

Boundary-layer bleed reduces the broad band noise by an amount which depends on the blade loading (nozzle size), location, and frequency. A reduction of as much as 12 decibels is produced at 0° with the 0.313-square-meter nozzle (fig. 10(a), 2.6 kHz); with the 0.330-square-meter nozzle, the reduction is generally much smaller (compare figs. 9 and 10). Increasing the bleed from 1.2 to 1.4 percent had negligible effects. In the rear quadrant ($\theta = 130^{\circ}$) the effects of boundary-layer bleed were negligible.

The spectrograms indicate that the broad band noise may be considered to contain a base level which declines at the rate of about 1.2 decibels per kilohertz (figs. 13 and 18 to 21). On this base are superimposed a number of discrete tones and broad band maxima:

A maximum in the 150- to 250-hertz region (figs. 7, 8, and 23 to 25)

A maximum in the 2.8-kilohertz region (figs. 9, 10, and 18 to 25)

A maximum in the 6.0- to 6.5-kilohertz region (figs. 10(b) to (d), 20(b), and 21(b))

These noise components are now discussed individually.

Low frequency noise. - The maxima in the broad band spectral density in the low frequency region of 150 to 250 hertz, displayed in the 1/3-octave bandwidth plots of figures 7, 8, show that the effect of bleed is to decrease this noise from 2 to 5 decibels with the large nozzle except for the 90^{o} microphone data. With the smaller nozzle, there is a consistent reduction in this noise with the minimum bleed, and no further gain is incurred by additional bleed. Low frequency broad band noise is generally thought to be generated in the jet, and the influence of the bleed on this noise is unexpected. It is therefore worthwhile to examine this noise in some detail. This examination gives evidence to show that the noise level and distribution differ substantially from pure jet noise produced by nozzle flow; therefore, other sources must be found to account for the data.

Experiments on the aerodynamic and acoustic properties of coaxial jets were reported by Williams, Ali, and Anderson (ref. 2). In their experiments the conditions differed from those of our tests. In theirs, the central or core jet was cold and the two jets emerged from the nozzles with no dead-air region between them; in the present tests, a 14-centimeter (5.5-in.) annular space existed between the two jets (fig. 5). The calculation methods of reference 2 give a maximum in the power spectrum (region of 50 to 70 Hz) this maximum is much lower than the engine jet data maximum in the 150- to 250-hertz region (fig. 14). According to the jet model of reference 2, the mixing and noise generation occur as a result of two processes: (1) mixing of the two jets at their mutual interface, and (2) mixing of the combined jet with the surrounding air. It is found that for the Lycoming engine the mixing of the two jets with each other dominates the noise production; therefore, the directional properties of the coaxial jet are determined by the source convection velocity at the interface of the two jets. In other words, the average of the two jet velocities is the convection velocity. The directional power distribution, which was calculated for a 16-hertz bandwidth at the maximum spectral density, is plotted in figure 15. In this calculation the overall power was calculated by the method of reference 2 for a coaxial jet using a constant suitable for turbulent inflow to the nozzle. The spectrum of that same source was used with the directional factor of $(1 + V_c \cos \theta/a_o)^{-5}$ (ref. 3). Also shown in figure 15 are the data for the measured maxima from 1/3-octave bandwidth spectrograms corrected to a 16-hertz bandwidth. The calculations are in rough agreement with the data near the jet at the back of the engine, but at the side and front, the calculations are much too low. Because of the large annular space between the jets, the geometry differed markedly from that of reference 2. The core jet was surrounded by a stagnant region; therefore, the calculations were also done for the core jet alone (assumed to be discharging into the atmosphere). The calculated frequency of the spectral maximum was found to be from 130 to 170 hertz, which agrees with the measurements. The peak sound pressure levels (16-Hz bandwidth) shown in figure 15 agree with the data measured at the engine discharge. The

single jet model also fails to account for the noise level measured near the front of the engine. Therefore, there is the probability that the low frequency noise near the front has a source other than the jet; it may arise in the fan itself.

In further support of this hypothesis are the data reported by Rice, Feiler, and Acker (ref. 4) and Groeneweg, Feiler, and Acker (ref. 5). When sound suppression equipment is placed in the fan housing, both of these tests show an unexpected reduction in the front quadrant of low frequency broad band noise (150- to 400-Hz range) in the amount of 2 to 7 decibels. This sound suppression equipment could only affect the radiation of noise being generated inside the fan, and one must assume the existence of some internal noise generation mechanism which may be operating in the present case as well. Reduction of low frequency noise by boundary-layer bleed might, therefore, as in the cases of the installation of sound absorbing materials, be the result of action on noise originating in the fan rather than in the jet.

There is also evidence to indicate that the level of noise generated in the jet can be influenced by the level of turbulence developed by the fan or engine which is cast into the jet (see Bushell, ref. 6). In the present circumstances, a reduction of fan nozzle size could cause the rotor blades to discharge larger blade wakes because of the increase in aerodynamic loading. (The diffusion factor increased from 0.36 to 0.47.) Removal of the casing boundary layer would improve conditions at the blade tips and reduce the spanwise extent of contamination of the blade boundary layer by flow from the blade tips. Thus, boundary-layer removal would reduce fan jet noise for highly loaded fan blading. (Compare fig. 7(f) with fig. 8(f).)

Boundary-layer turbulence noise. - When rotor blade tips are immersed in the turbulent flow of the boundary layer on the case, they will be buffeted by small velocity fluctuations normal to the blade surfaces (upwash perturbations). These will cause fluctuations in the angle of attack on the blades and therefore in the blade lift force. Such a fluctuating force acting on the fluid causes acoustic radiation. According to Sharland (ref. 7, eq. (5)) the acoustic power radiated by an airfoil in a turbulent stream is

$$W = \frac{\rho_o}{48\pi a_o^3} \int cV^4 S_c \left\langle \left(\frac{\partial C_L}{\partial t} \right)^2 \right\rangle dy \qquad (1)$$

where

C_L fluctuation of lift coefficient of airfoil section

S_c area of correlation of surface pressure fluctuations

V mean stream velocity in turbulent flow

$\langle\rangle$ time average

When expressing this result in terms of turbulence, Sharland calculates

$$\frac{\partial C_L}{\partial t} = \left(\frac{\partial C_L}{\partial \alpha}\right)\left(\frac{\partial \alpha}{\partial t}\right)$$

where α is the fluctuation of the flow angle from the mean value. Because he does not take into account the fall-off of airfoil response C_L (lift coefficient) as the frequency of the turbulence increases, he calculates too high a radiation level. The theory can be modified by using Sears' results for sinusoidal gusts (ref. 8). Thus, if we regard the fluctuation of the lift coefficient as decomposed into frequency components,

$$C_L(t) = 2\pi \frac{w_o}{V} e^{i\omega t} \varphi(k) \tag{2}$$

where t is time, w_o upwash amplitude component in frequency range w to w + dw, and

$$w = w_o e^{i\omega t} \quad \text{turbulence velocity (upwash)}$$

$$k = \frac{\omega c}{2V} = \frac{\pi f c}{V}$$

In equation (2) the function $\varphi(k)$ produces a reduced amplitude as the frequency increases. The equation shows that

$$\frac{\partial C_L}{\partial t} = i\omega C_L \tag{3}$$

and

$$\left\langle \left(\frac{\partial C_L}{\partial t}\right)^2 \right\rangle = \omega^2 \left\langle C_L^2 \right\rangle \tag{4}$$

Sharland introduces a plausibility argument to show that

$$\omega^2 S_c = K_1 V^2$$

where K_1 is some constant. The radiated power is then

$$W = K_2 \int_{Span} CV^6 \left\langle C_L^2 \right\rangle dy \tag{5}$$

When the gusts are turbulent, rather than sinusoidal, the fluctuation of the mean-square lift coefficient is shown by Liepmann (ref. 9) to be

$$\left\langle C_L^2 \right\rangle = 4\pi^2 \int_0^\infty d\omega \left[\psi_w(\omega) \left| \varphi(\omega) \right|^2 \right] \tag{6}$$

where $\psi_w(\omega)$ is the power spectral density of w/V. Furthermore, Liepmann has shown that a good approximation for $\left| \varphi(\omega) \right|^2$ is

$$\left| \varphi(\omega) \right|^2 = \frac{1}{1 + \pi\omega c/V} \tag{7}$$

If an average value of the integrand is used over the portion of the blade span emitting noise, then we have a further modification of Sharland's equation from

$$W = K_3 C \int_{Span} dy \left\{ V^6 4\pi^2 \int_0^\infty d\omega \left[\frac{\psi_w(\omega)}{1 + \pi\omega c/V} \right] \right\} \tag{8}$$

to

$$W = K_4(Span) \int_0^\infty d\omega \frac{\psi_w(\omega)}{1 + (\pi c/V)\omega} \tag{9}$$

Therefore, the spectral density of the airfoil radiation corresponding to equation (9) is

$$\frac{dW}{df} = K_5(Span) \frac{\psi_w(f)}{(1 + 2\pi^2 cf/V)} \tag{10}$$

An effective span for acoustic radiation can be estimated from the distribution of the radiation intensity from equation (8) (ref. 7), which shows the important criterion to be the distribution of $\langle w^2 \rangle V^4$. The data of Serafini (ref. 10) show that $\langle w^2 \rangle V^4$ and airfoil acoustic radiation reach a maximum in the region of the boundary layer specified as

$0.06 \leq y/\delta \leq 0.24$ (where $0.83 \leq V/V_o \leq 0.94$) and that substantial power is being radiated from $y \cong \delta$ (δ, boundary-layer thickness). At larger distances from the wall, power drops rapidly with $\langle w^2 \rangle$. Consequently, the boundary-layer thickness δ may be taken as the distance within which the blade radiates acoustically. The span of the blade within this distance is $(\delta - \Delta)$, where Δ is the blade-tip clearance space.

The only additional requirement for comparison of the spectrum of equation (10) with the data is the spectral function ψ_w. The wall surface pressure data of M. K. Bull (ref. 11) has been used for this purpose, since it is believed that the processes producing pressure fluctuation at the wall and at the airfoil are very similar except for the influence of the airfoil response function $\varphi(k)$. Thus, the airfoil radiation spectrum would seem to be reasonably approximated by

$$\frac{dW}{df} = \frac{K_5(\delta - \Delta)\psi_p(f)}{(1 + 2\pi^2 cf/V)} \tag{11}$$

where

$$\frac{d\left\langle P_w^2 \right\rangle}{df} \equiv \psi_p(f)$$

and P_w is the pressure fluctuation at the wall. In further support of this substitution is the demonstration by Kraichnan (ref. 12) that the wall pressure fluctuation is nearly proportional to the turbulence-shear terms $w_\alpha V_\beta$, where α and β are running coordinate indexes. Therefore, the pressure spectrum is proportional to the turbulence spectrum, since p and w are approximately linearly related. The data of reference 11 are presented in generalized (dimensionless) parameters so that dependence on specific boundary-layer conditions can be explicitly shown. With $f\delta^*/V_o$ as the generalized (dimensionless) frequency, the generalized spectral density is given by

$$Q(f\delta^*/V_o) \equiv \frac{4\psi_p(f)}{\rho^2 V_o^3 \delta^*} \tag{12}$$

and

$$\frac{dW}{df} = \frac{K_6 \delta^* (\delta - \Delta) Q(f\delta^*/V_o)}{1 + f/150} \tag{13}$$

This equation shows that reduction of the boundary-layer thickness reduces the intensity of the radiation by a factor of $\delta^*(\delta - \Delta)$. It also shifts the frequency distribution of the spectrum to higher values because equal values of the dimensionless frequency argument $f\delta^*/V_o$ require higher frequencies f. The precise value of δ appropriate to the $\langle w^2 \rangle$ distribution is not known in the present tests. However, an estimate is made from the measured distributions by assuming a power-law velocity distribution:

$$\frac{V}{V_o} = \left(\frac{y}{\delta}\right)^n \tag{14}$$

A value of $\delta = 8.5$ millimeters can be obtained from equation (14) when $\delta^* = 3.53$ millimeters and $\theta^* = 1.45$ millimeters. At this distance from the wall, the measurements show that $V/V_o = 0.94$. When the inner layer is sucked out (1.2 percent suction), then $V/V_o = 0.94$ at the point $y = 5.3$ millimeters. Curves of the radiation spectrum dW/df are shown in figure 16 in relative decibel units for these two cases.

The theoretical spectral distribution was modified to include the effect of the line impedance in order to render a simpler comparison of the recorded data with the calculation data (compare fig. 16 with figs. 18 to 21). The curves have shapes roughly similar to those of the base level of the broad band noise, provided the maxima are discounted at 250 hertz, and 2.8 and 6.2 kilohertz. The reduction in broad band noise base level with reduction of boundary-layer thickness supports the hypothesis that this noise results from the interaction of the blades with the casing boundary layer.

Vortex shedding noise - blade trailing edges. - The maxima in the broad band spectral density near 2.8 and 6.2 kilohertz are thought to result from two types of vortex shedding. Vortex shedding from the trailing edges of rotor or stator blades was discussed by Sharland (ref. 7) as a source of noise in fans. At sufficiently high Reynolds numbers there is discharged from the trailing edge of the blades a mixture of vortices and turbulence which produce a broad band noise from sources in the wake and on the blade. This noise is characterized by a spectrum having a density at some characteristic frequency. This mechanism was advanced by Sharland (ref. 7). A dimensionless form of the characteristic frequency is the Strouhal number $S = fL/V$ where L is some characteristic length scale. As one considers the portions of the blade closer to the hub, the relative velocity is smaller and the whole noise spectrum shifts to lower frequencies. Thus, the overall radiation of this type from the blades is rather complex, but it should be dominated by conditions near the blade tips because of the higher velocity there. Sharland uses the blade thickness as a characteristic scale for the Strouhal number, but this seems to be an irrelevant choice. Experimental data on noise spectrums reported by Roshko (ref. 13) were correlated for several cylinder shapes using a Strouhal number based on wake thickness and stream velocity at the flow separation

point. The approach velocity will be used to approximate the value at the separation point.

The thickness L of the airfoil wake may be estimated as

$$L = 2\delta + t_e \tag{15}$$

where t_e is the trailing edge thickness. For the turbulent boundary layer, with a 1/7-power velocity distribution,

$$\delta \approx 10\theta^*$$

where θ^* is the momentum thickness. The momentum thickness can be estimated from the airfoil loss coefficient:

$$2\theta^* \approx \overline{\omega} X \cos \beta_2 \tag{16}$$

(ref. 14, in the limit of $\theta^* << X$) where β_2 is the air flow angle at the trailing edge of a blade relative to the machine axis and X is blade pitch (distance between corresponding points on adjacent blades, 7.6 cm at the blade tips). A common midspan range of values of $\overline{\omega}$ is 0.02 to 0.03 (ref. 15). Then, for the fan rotor blades, θ^* is approximately 0.38 to 0.56 millimeter (0.015 to 0.022 in.) and the wake width L is from 8.4 to 12.0 millimeters (by eq. (15)). For a Strouhal number of 0.164 (ref. 13), the characteristic frequency is 6300 hertz $\geq$ f $\geq$ 4400 hertz at the blade tips. At the inner radius of the fan blades, the characteristic frequency would be lower if this section were isolated from the remainder of the blade. However, the stronger impulses come from near the blade tips, and this region is probably the most important in determining the characteristic frequency of the vortex shedding process.

Because this noise is generated over an extensive region of the blade span, the effect of removing the boundary layer on the casing should be negligible. The effect of nozzle size should not be negligible; a small nozzle increases the work on the gas and the aerodynamic loading of the rotor blades. Increasing the blade loading increases the blade surface pressure gradients, the boundary-layer thickness, and the thickness of the blade wakes. The larger wakes develop larger vortices and larger pressure fluctuations on the blade and in the wake, and, therefore, more noise develops with the small nozzle. When the fan is operated with the larger nozzle, the maximum in the 5.5- to 6.5-kilohertz region is not clearly shown (fig. 7); with the smaller nozzle there is a prominent maximum at locations $\theta = 30^\circ$, 40°, and 50°. The maximum spectral density values in the 5.5- to 6.5-kilohertz frequency region are given in table III.

TABLE III. - MAXIMUM SPECTRAL DENSITY BETWEEN 5.5 AND 6.5 KILOHERTZ[a]

Bleed, percent	Position, deg					
	0	30	40	50	90	130
	Density, dB/Hz					
0	72	77	78	76	73	73
1.2	72	77	77	82	73	73
1.4	73	81	80	80	74	73

[a]Bandwidth, 64 Hz; fan nozzle area, 0.313 m^2.

These data exhibit no consistent and substantial effect of bleed and therefore indicate that the noise source producing the broad band maximum in the 6 kilohertz region is not connected with the boundary layer on the casing; the variation with loading and the characteristic frequency range suggest that vortex shedding from the rotor blade trailing edges produces the noise.

Vortex shedding noise - blade tips. - Flow separation from the blade tips is normally expected without boundary-layer bleed because of the very high angle of attack on the blade, which results from the low axial velocity of the gas in the boundary layer on the fan casing and the high rotational velocity of the blade. Noise produced by these separation vortices should be subject to control by the boundary layer on the casing. The separation here may extend from the leading edge of the blade; its spanwise extent is not limited to the boundary-layer region, but should extend to adjacent regions where the blade surface boundary layer must pass through a large pressure rise, because of spanwise flows of the boundary layer. This noise must be sensitive, therefore, to loading the blades as well as boundary-layer removal. The characteristic frequency might be estimated as previously by using the wake thickness as the length scale. The wake can be no thicker than the normal distance between blades; this scale gives a typical frequency of 2050 hertz. The observed maximum in the region of 2600 to 3000 hertz would correspond more precisely to the process of separation of the flow from the leading edges of the blades if the interblade channels were only partially filled with the wake. The wake thickness would vary along the span.

These maxima are displayed in figures 18 to 21, and additional details shown in the 16-hertz bandwidth plots of some of these data in figures 22 to 25. Comparison of the effect of varying operating conditions on the amplitude of this noise component is facilitated by the summary in figure 17, which shows the peak amplitude in this frequency range selected from figures 18 to 21, 9, and 10 (64-Hz bandwidth). This noise increases by 10 to 12 decibels in the 0° to 30° region when the nozzle size is reduced; at

the side of the engine the increase is not so large. When the casing boundary layer is removed, the front noise is decreased to the level observed with the larger nozzle. Bleeding off the boundary layer does not reduce this front noise when the larger fan nozzle is used. These data lend credibility to the hypothesis that there is a separation of the flow from the blade tip at or near the leading edge, associated with a vortex shedding process and noise production, and furthermore, that this separation at the blade tips triggers a large spanwise effect in highly loaded blades but has a small effect on lightly loaded blades.

System noise. - An effect not previously noted appears in the data obtained from the microphone located at 130°; in the frequency range of 1 to 2 kilohertz (see figs. 9(f) and 10(f)), the noise increases as the boundary layer is bled off. This noise probably originates in the ejector of the bleed system and is therefore not so prominently displayed in the noise spectrum from the microphones more remote from the ejector.

SUMMARY OF RESULTS

The thickness of the boundary layer on the casing of the fan of the Lycoming turbofan engine was reduced by means of an external bleed system. The outlet guide vanes were removed to obtain knowledge of the acoustic effects of rotor interaction with this boundary layer without interference from the outlet guide vanes.

Boundary-layer bleed produced a small reduction in blade passing tone. In a complete stage the effect would be greater for a subsonic rotor and perhaps less for a transonic rotor because of the dominance of the blade shock noises which are unaffected by bleed.

The broad band spectrum density decreases gradually with increasing frequency; superimposed on it are maxima located at 150 to 250, 2800, and 6200 hertz. The broad substratum component is reduced as much as 7 decibels in special circumstances by bleeding off the boundary layer. The spectrum of this noise and its relation to boundary-layer thickness indicate that it is probably caused by the acoustic reaction of rotor blade tips to turbulence in the casing boundary layer.

The low frequency maximum (150 to 250 Hz) was reduced from 2 to 5 decibels when the boundary layer was removed and the fan was operating with the large nozzle. When the fan was operating with the small nozzle, the reduction in noise is slightly larger. When 1.2 percent of the flow is bled from the casing additional suction does not reduce this noise further. This noise is believed to be partly generated in the fan jet and to depend on the level of turbulence cast into that jet by the rotor. Additionally, internal sources of this noise are indicated by the high level of the noise propagated forward, as compared with the propagation pattern of a pure jet.

The maximum in the region of 2800 hertz is increased 12 decibels in the forward sector by increasing the loading of the rotor blades. This noise increase can be eliminated by bleeding off sufficient air so that the rotor blade tips do not project into the casing boundary layer. This noise is thought to originate in the process of flow separation and vortex shedding from the suction surfaces of the blades near the tips, either at leading edge or at some other point well forward of the trailing edge.

The noise maximum at 6300 hertz did not correlate with boundary-layer bleed. It did increase with blade loading and is believed to originate in vortex shedding from the rotor blade trailing edges, along the entire blade span.

Lewis Research Center,
National Aeronautics and Space Administration,
Cleveland, Ohio, January 27, 1972,
132-80.

REFERENCES

1. Acker, Loren W.; Balombin, Joseph R.; and Coats, James W.: Sound Measurements on a 4000-Pound-Thrust High-Bypass-Ratio Turbofan Engine. NASA TM X-1950, 1970.

2. Williams, T. J.; Ali, M. R. M. H.; and Anderson, J. S.: Noise and Flow Characteristics of Coaxial Jets. J. Mech. Eng. Sci., vol. 11, no. 2, Apr. 1969, pp. 133-148.

3. Ffowcs-Williams, J. E.: Some Thoughts on the Effects of Aircraft Motion and Eddy Convection on the Noise from Air Jets. USAA Rep. 155, Univ. Southampton, Sept. 1960.

4. Rice, Edward J.; Feiler, Charles E.; and Acker, Loren W.: Acoustic and Aerodynamic Performance of a 6-Foot Diameter Fan for Turbofan Engines. III - Performance with Noise Suppressors. NASA TN D-6178, 1971.

5. Groeneweg, John F.; Feiler, Charles E.; and Acker, Loren W.: Inlet Noise Suppressor Performance with a Turbojet Engine as a Noise Source. NASA TN D-6395, 1971.

6. Bushell, K. W.: A Survey of Low Velocity and Coaxial Jet Noise with Application to Prediction. Symposium on Aerodynamic Noise, Loughborough University, Eng., Sept. 14-17, 1970, pp. B.3.1.-B.3.23.

7. Sharland, I. J.: Sources of Noise in Axial Flow Fans. J. Sound Vib., vol. 1, no. 3, July 1964, pp. 302-322.

8. Sears, William R.: Some Aspects of Non-Stationary Airfoil Theory and Its Practical Application. J. Aeron. Sci., vol. 8, no. 3, Jan. 1941, pp. 104-108.

9. Lieppmann, H. W.: On the Application of Statistical Concepts to the Buffeting Problem. J. Aeron. Sci., vol. 19, no. 12, Dec. 1952, pp. 793-800, 822.

10. Serafini, John S.: Wall-Pressure Fluctuations and Pressure-Velocity Correlations in a Turbulent Boundary Layer. NASA TR R-165, 1963.

11. Bull, M. K.: Boundary Layer Pressure Fluctuations. Noise and Acoustic Fatigue in Aeronautics. E. J. Richards and D. J. Mead, eds., John Wiley & Sons, Inc., 1968, pp. 169-180.

12. Kraichnan, Robert H.: Pressure Fluctuations in Turbulent Flow Over A Flat Plate. J. Acoust. Soc. Am., vol. 28, no. 3, May 1956, pp. 378-390.

13. Roshko, Anatol: On the Drag and Shedding Frequency of Two-Dimensional Bluff Bodies. NACA TN 3169, 1954.

14. Roudebush, William H.; and Lieblein, Seymour: Viscous Flow in Two-Dimensional Cascades. Aerodynamic Design of Axial-Flow Compressors. Irving A. Johnsen and Robert O. Bullock, eds., NASA SP-36, 1965, pp. 151-181, eqn. 260.

15. Lieblein, Seymour: Experimental Flow in Two-Dimensional Cascades. Aerodynamic Design of Axial-Flow Compressors. Irving A. Johnsen and Robert O. Bullock, eds., NASA SP-36, 1965, pp. 183-226, figs. 152, 155.

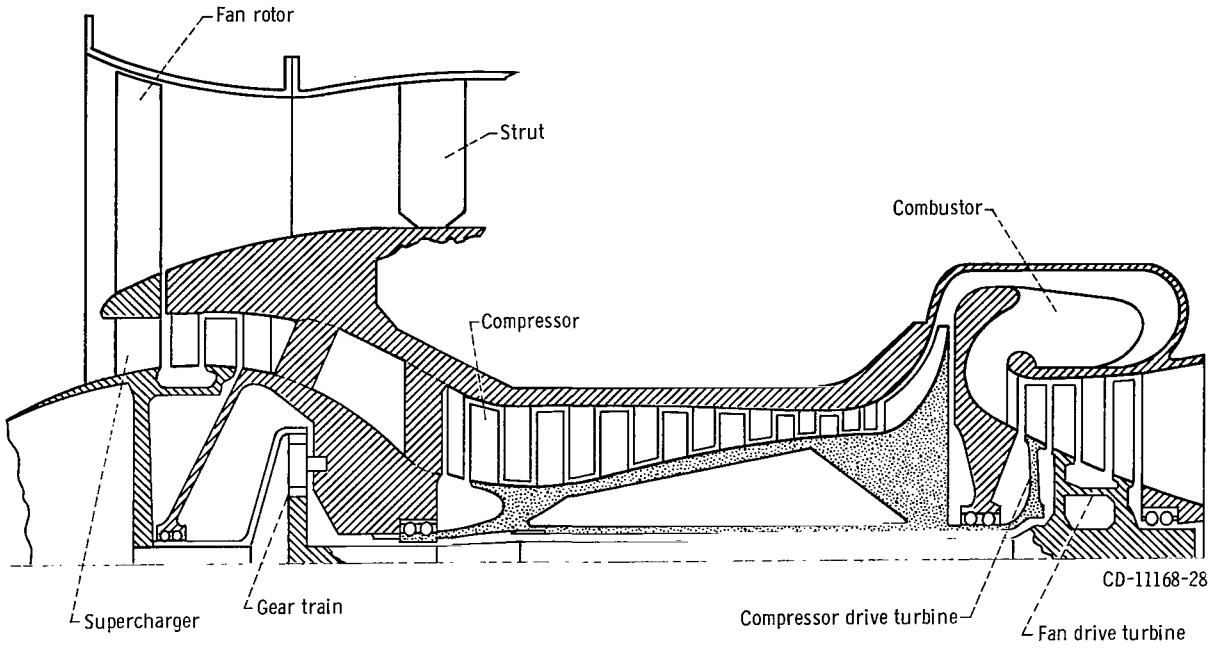

Figure 1. - Schematic diagram of core engine and fan rotor.

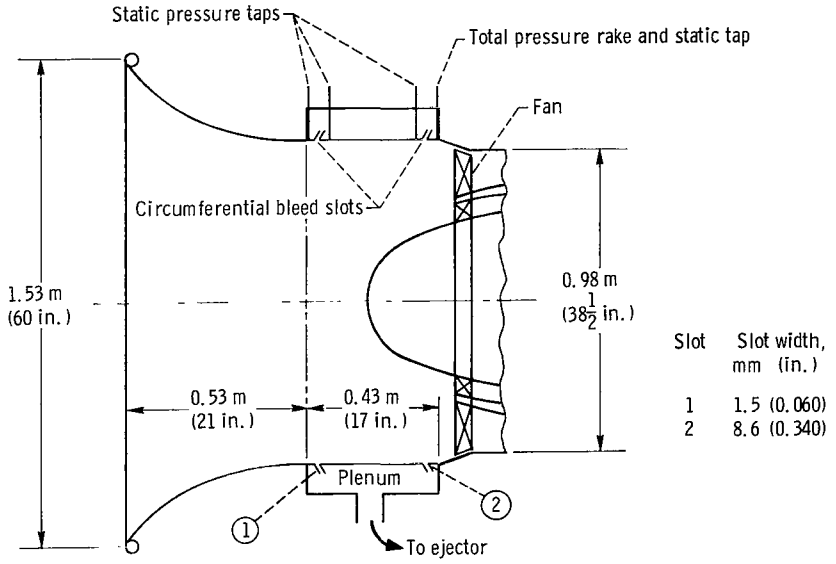

Figure 2. - Schematic of boundary layer bleed arrangement.

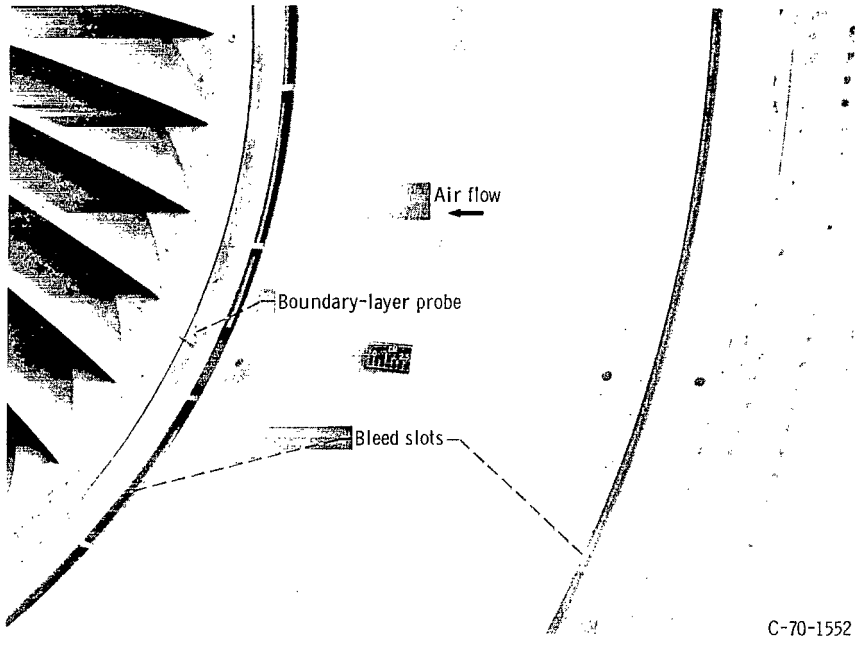

Figure 3. - Inlet duct and rotor blading.

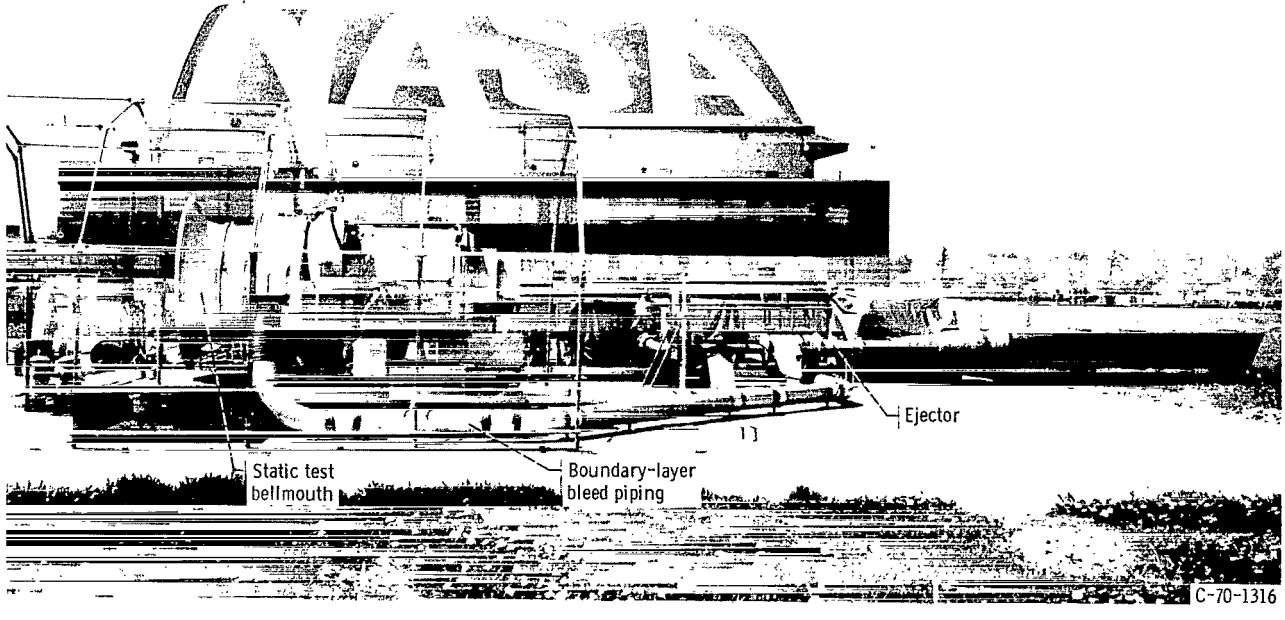

Figure 4. - Turbofan engine with static inlet and bleed ejector system.

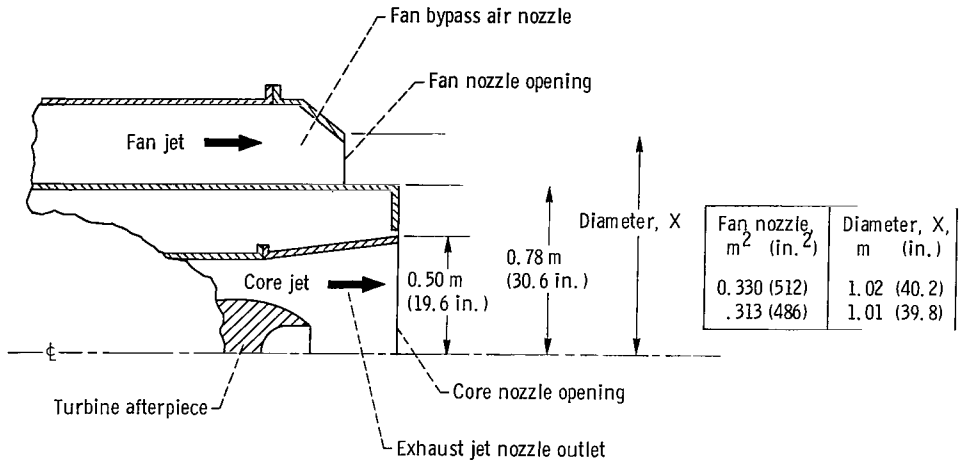

Figure 5. - Schematic of exhaust nozzles of fan and core jets.

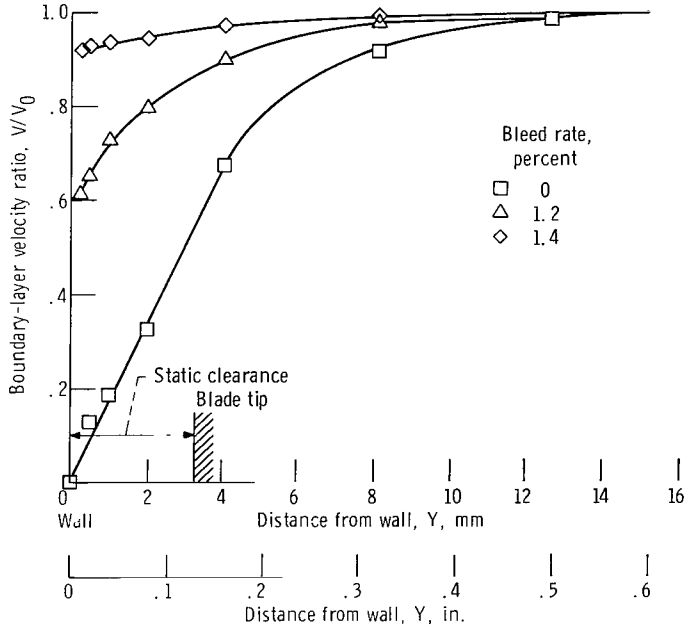

Figure 6. - Velocity in boundary layer on fan casing 38 millimeters upstream of rotor blading.

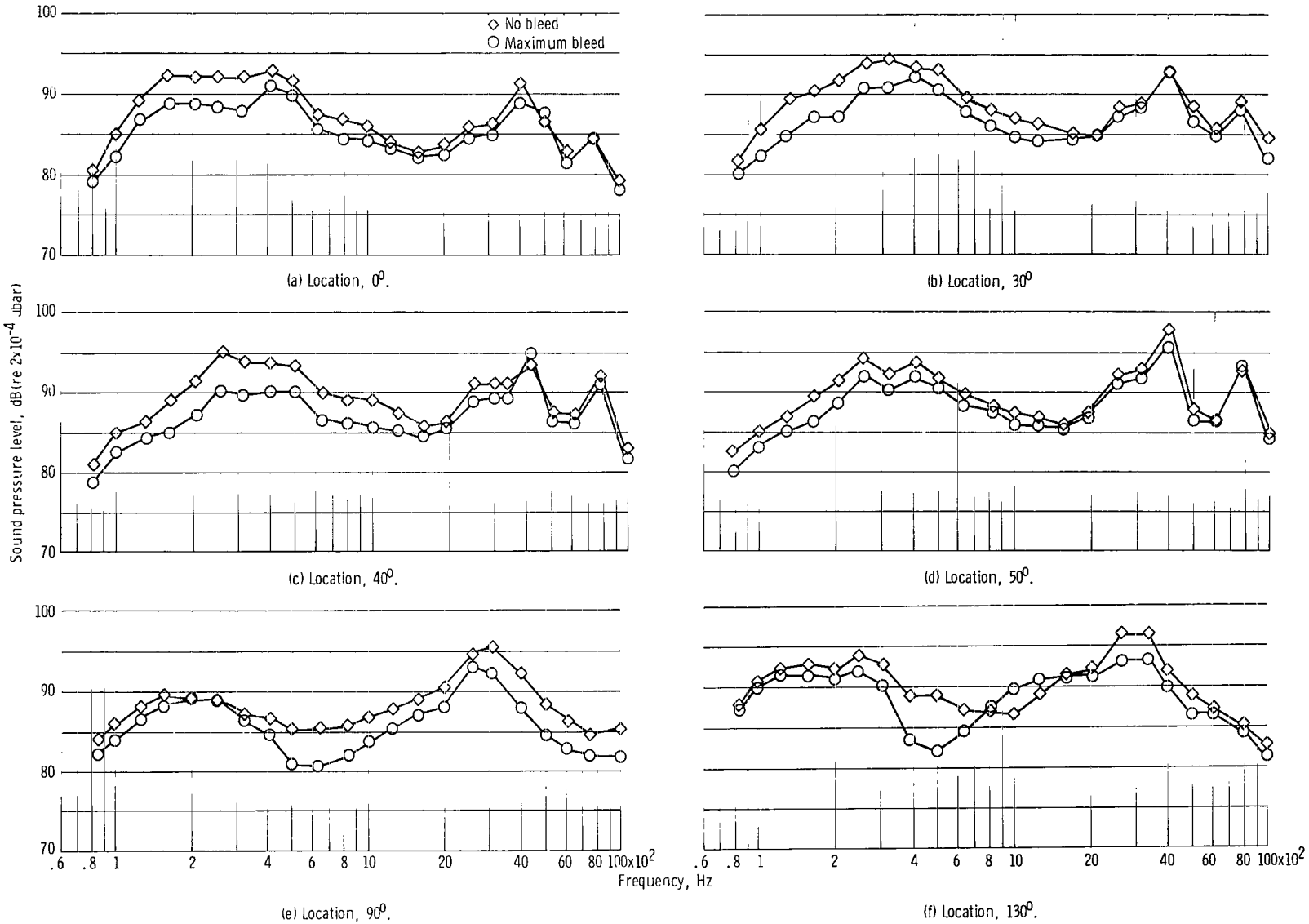

Figure 7. - Engine spectrogram. Nozzle, 0.330 square meter (512 in.^{2}); 1/3-octave bandwidth.

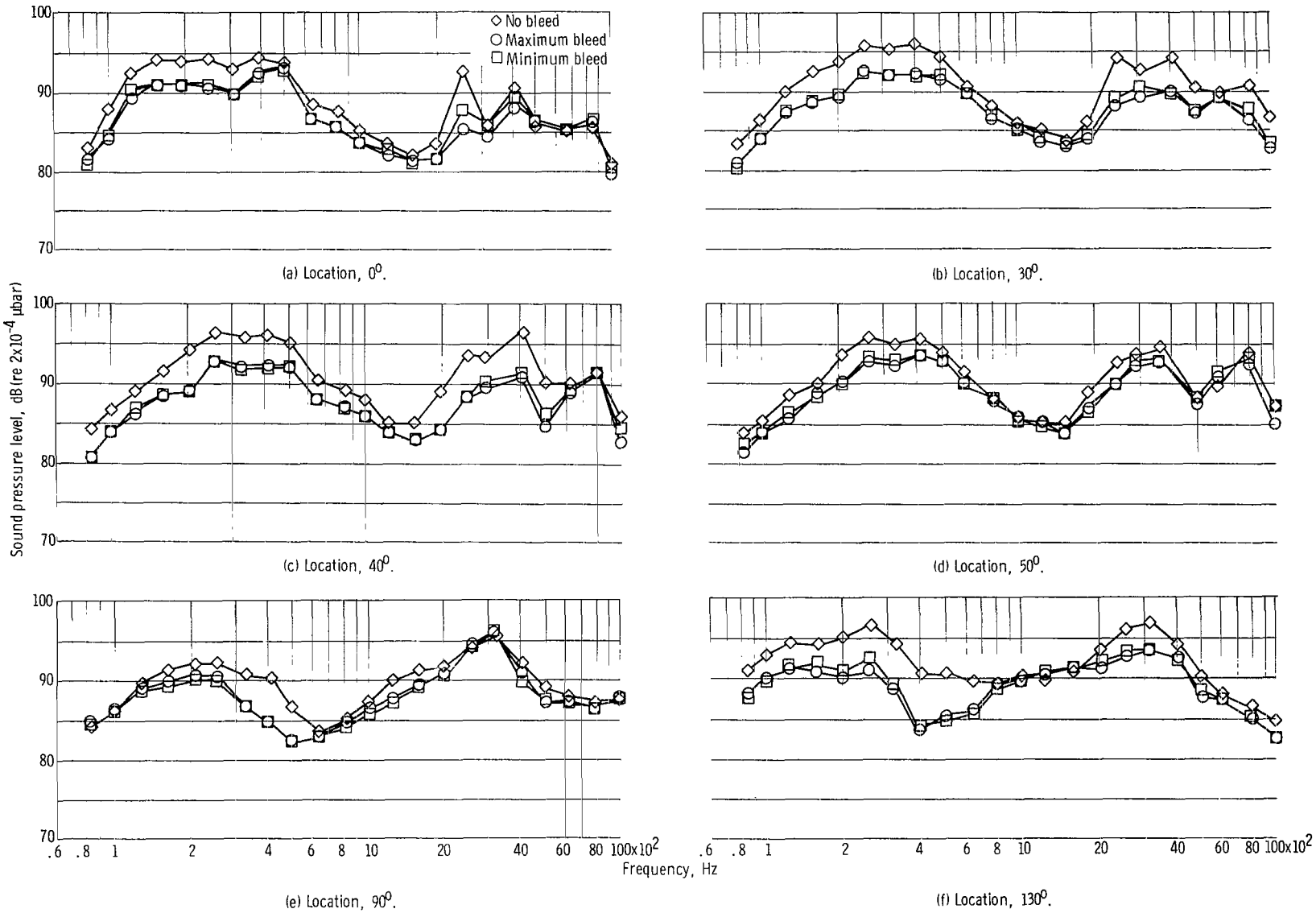

Figure 8. - Engine spectrogram. Nozzle, 0.313 square meter (486 in.^{2}); 1/3-octave bandwidth.

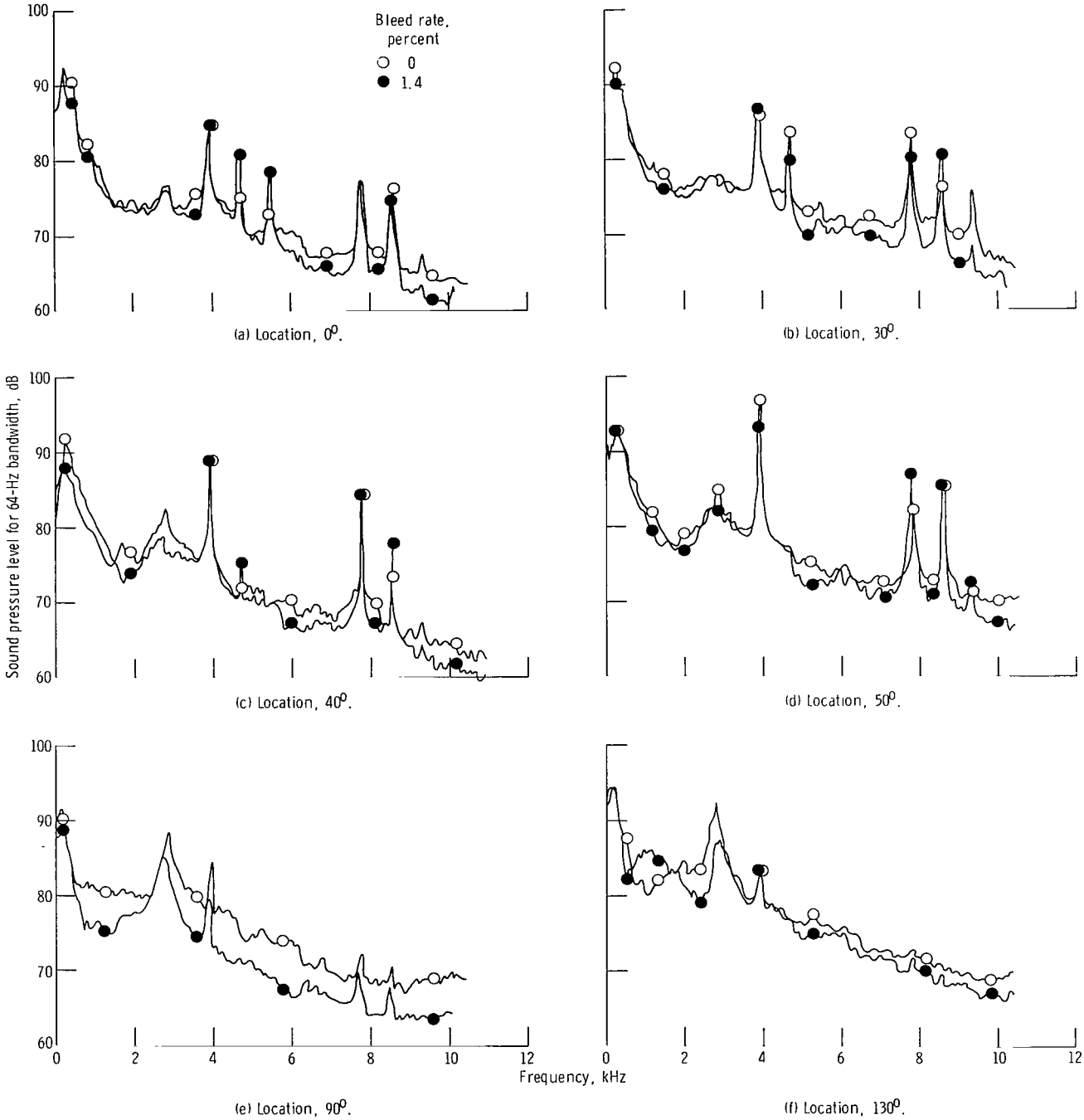

Figure 9. - Effect of bleed on spectrograms with 0.330 square meter (512 in.^{2}) fan nozzle.

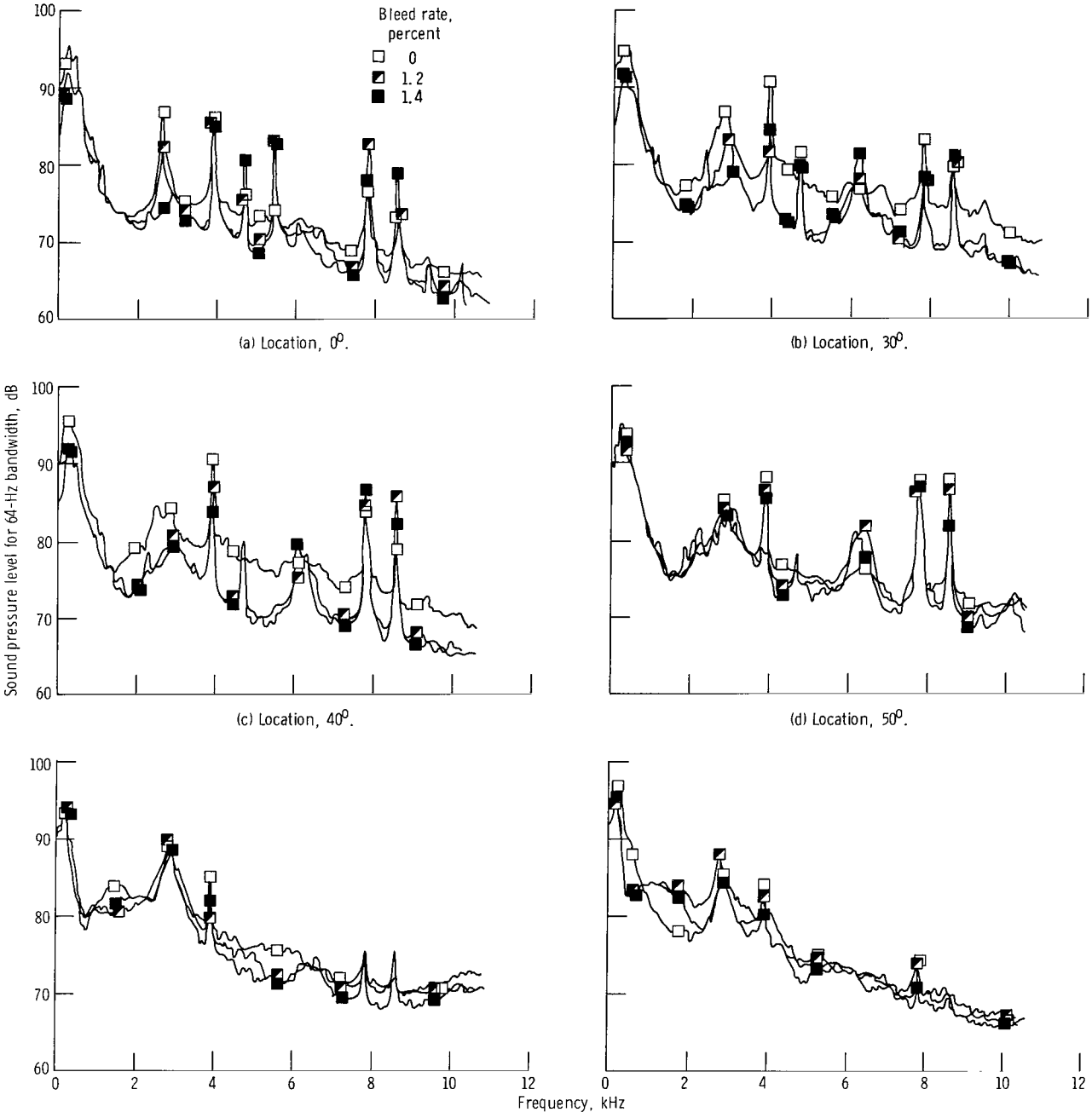

Figure 10. - Effect of bleed on spectrograms with 0.313 square meter (486 in.^{2}) fan nozzle.

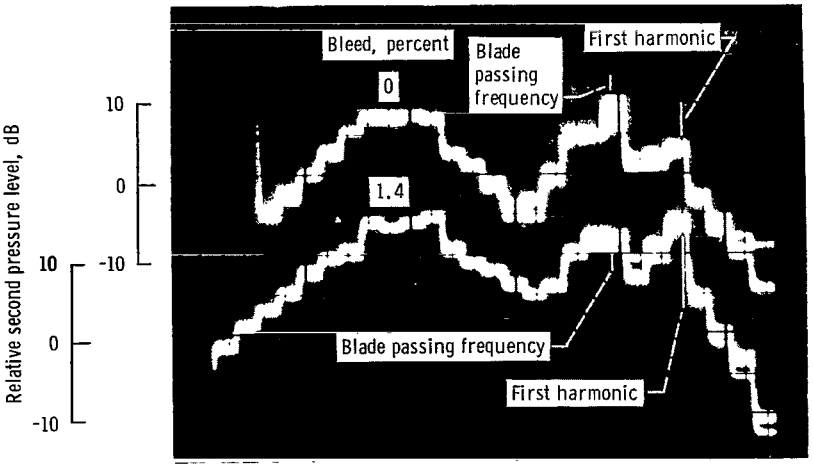

Figure 11. - Spectrograms (12 superimposed). One-third-octave bandwidth; 4-second samples.

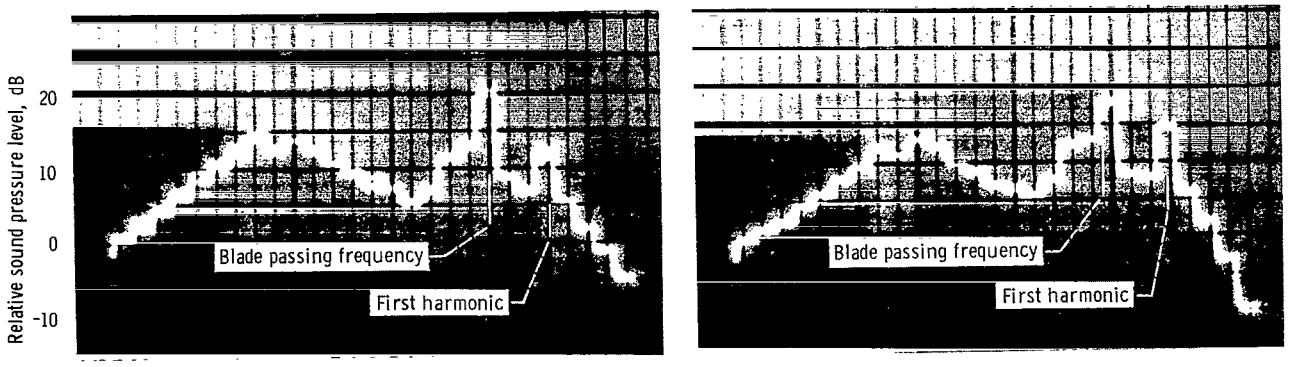

(a) Bleed, 0 percent.

(b) Bleed, 1.4 percent.

Figure 12. - Spectrograms (4 superimposed). One-third-octave bandwidth; 32-second samples.

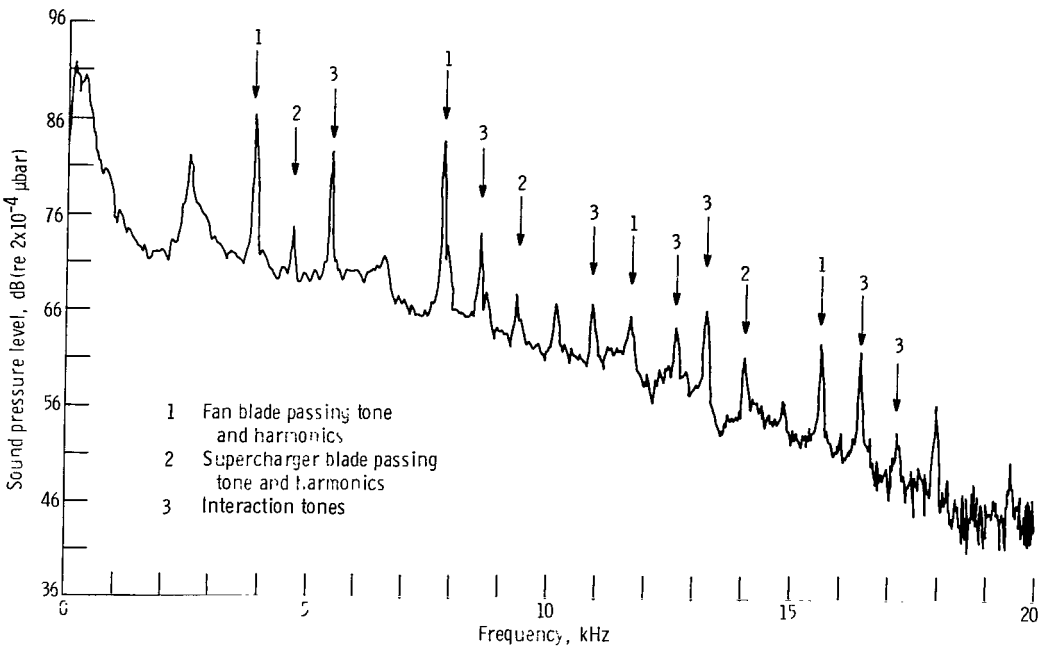

Figure 13. - Spectrogram showing discrete tone system (64 Hz bandwidth).

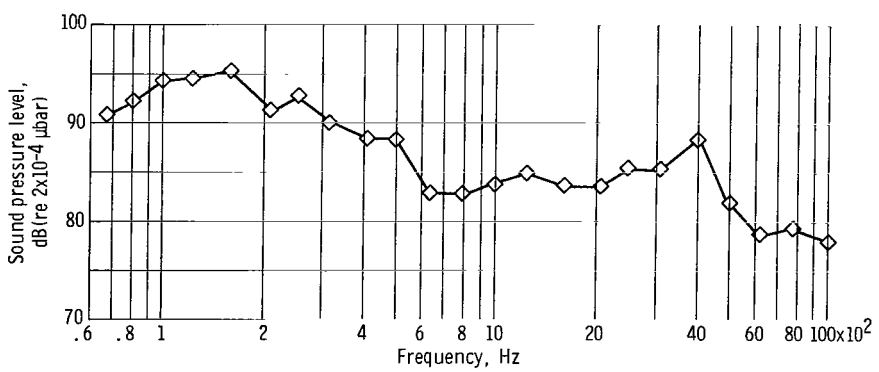

Figure 14. - Spectrogram of jet noise with no bleed. Nozzle, 0.330 square meter (512 in.^{2}); 1/3-octave bandwidth; location, 160°.

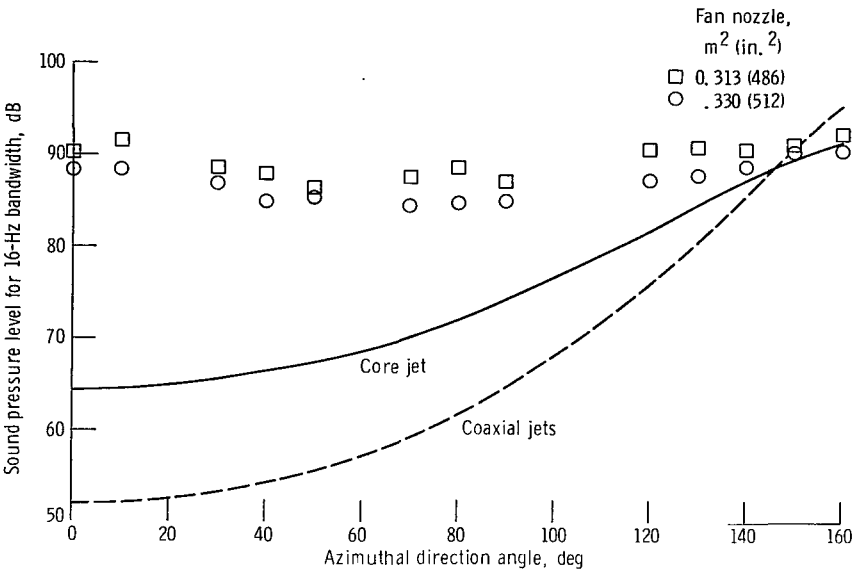

Figure 15. - Distribution of low frequency noise (160 Hz) for engine and maximum spectral density for estimated jet noise.

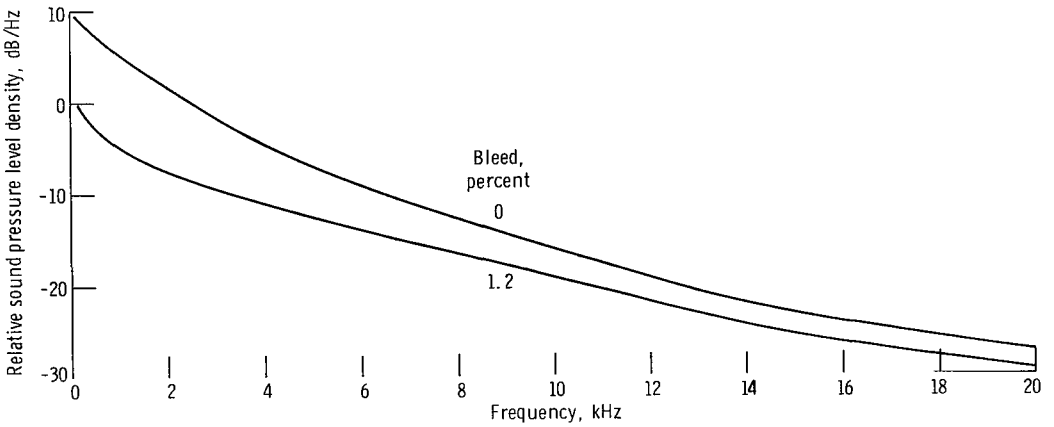

Figure 16. - Estimated spectral density with airfoil tip in boundary layer.

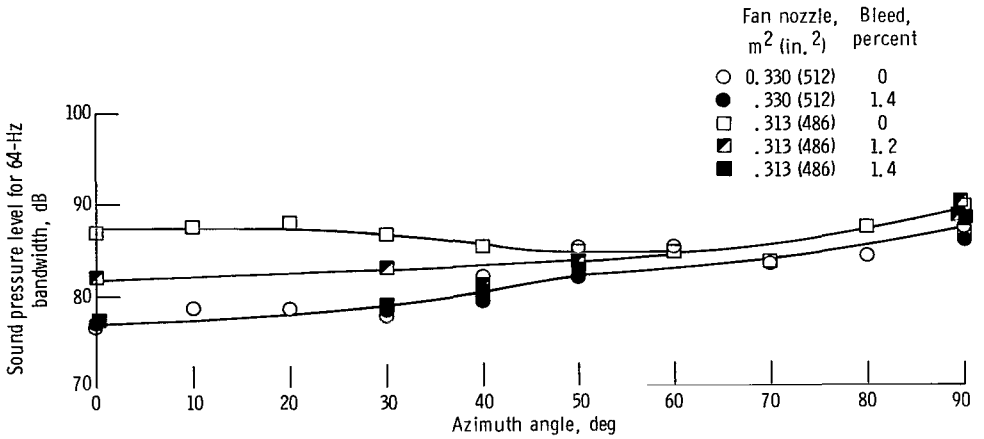

Figure 17. - Distribution of spectral maximum in 2600 to 3000 hertz range.

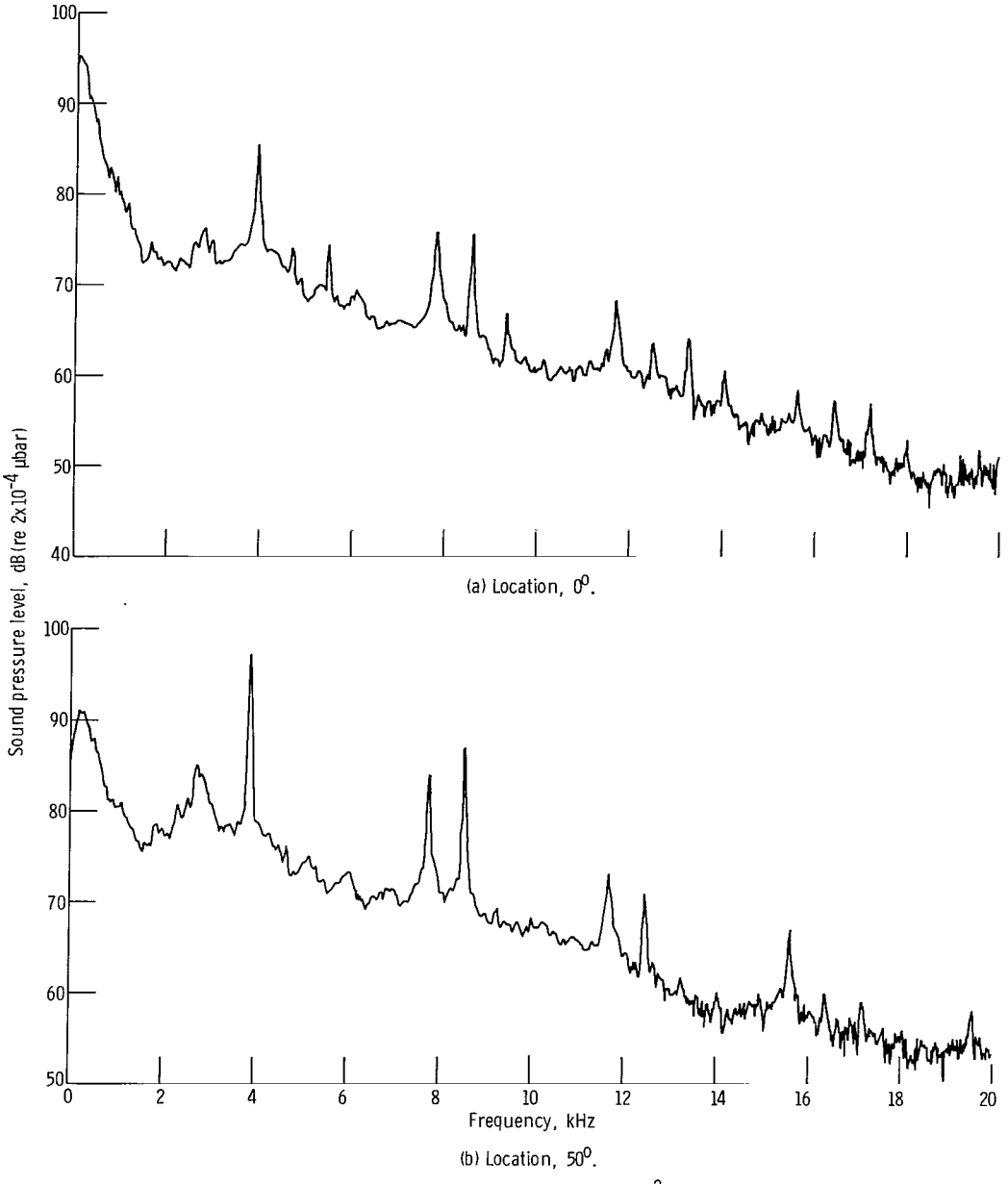

Figure 18. - Engine spectrogram. Nozzle, 0.330 square meter (512 in.^{2}); bandwidth, 64 hertz; bleed rate, 0 percent.

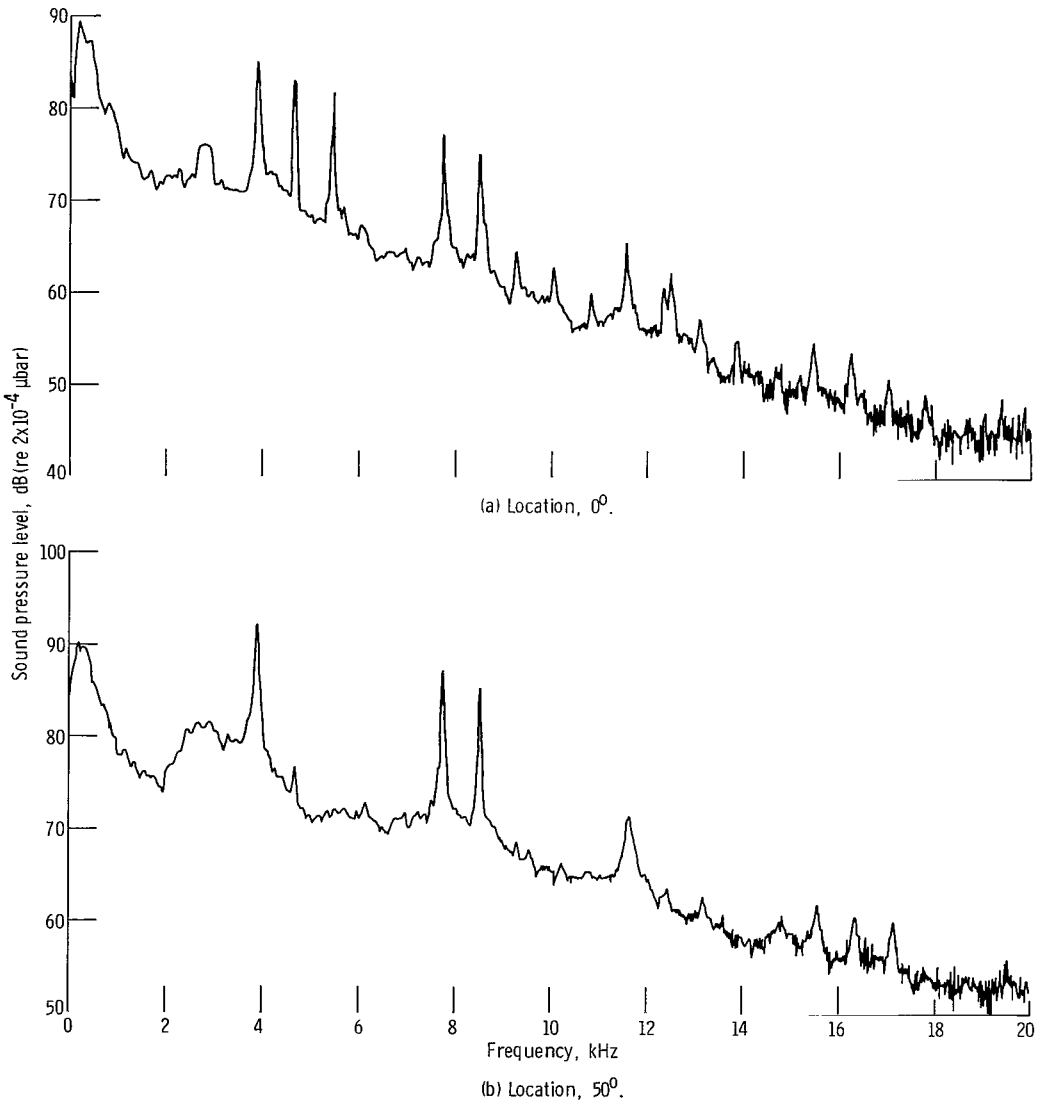

Figure 19. - Engine spectrogram. Nozzle, 0.330 square meter (512 in.^{2}); bandwidth, 64 hertz; bleed rate, 1.4 percent.

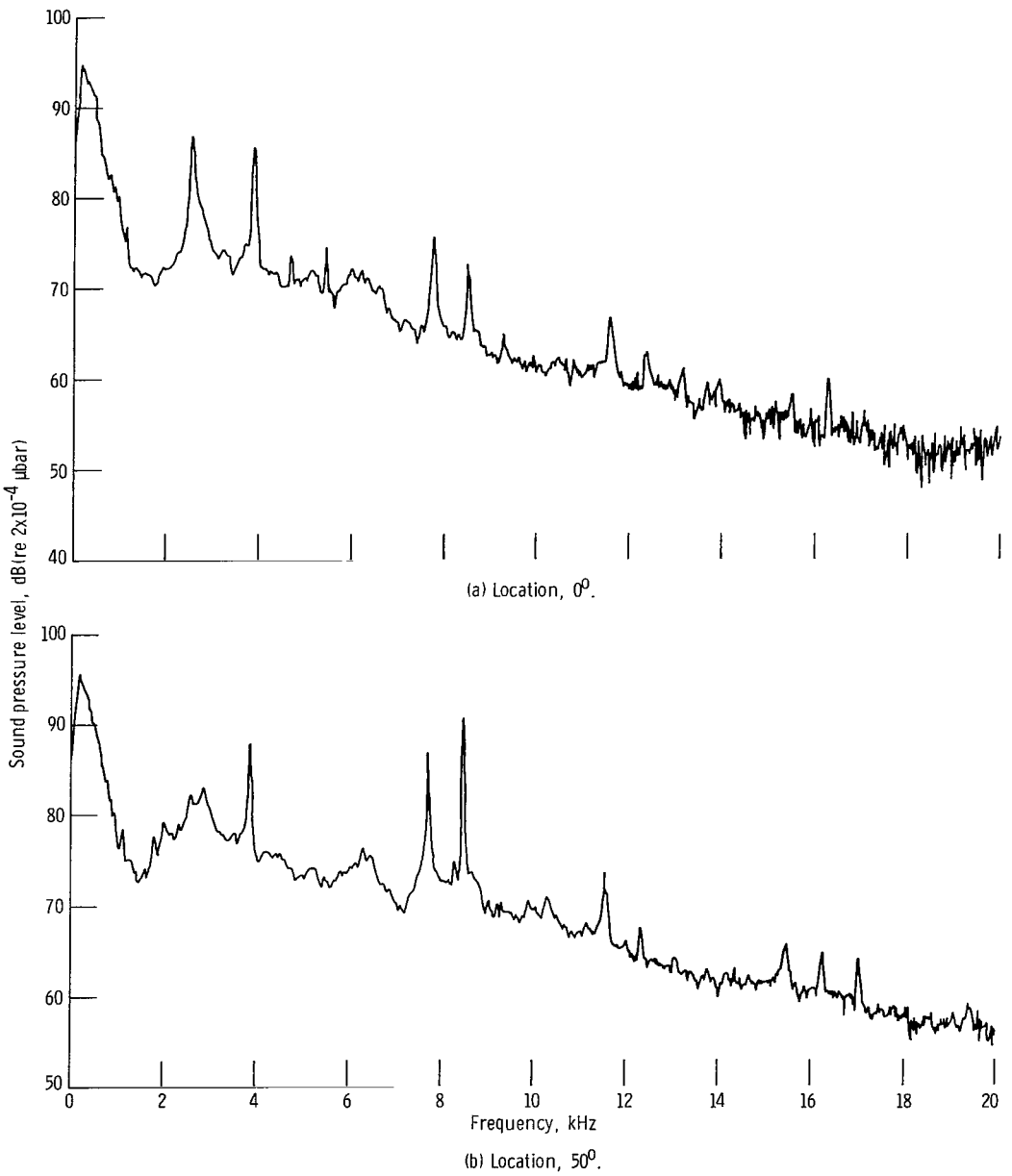

Figure 20. - Engine spectrogram. Nozzle, 0.313 square meter (486 in.^{2}); bandwidth, 64 hertz; bleed rate, 0 percent.

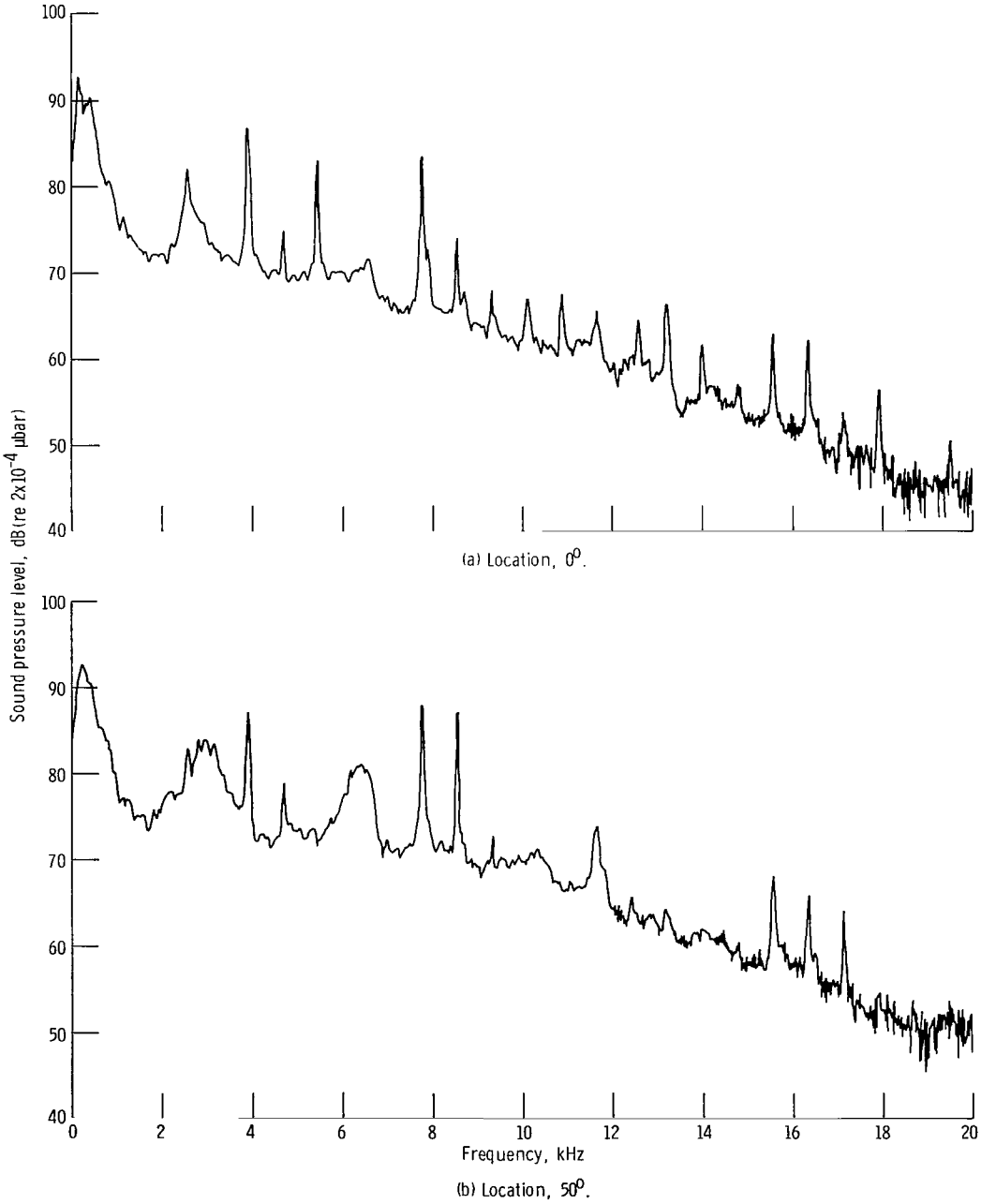

Figure 21. - Engine spectrogram. Nozzle, 0.313 square meter (486 in.^{2}); bandwidth, 64 hertz; bleed rate, 1.2 percent.

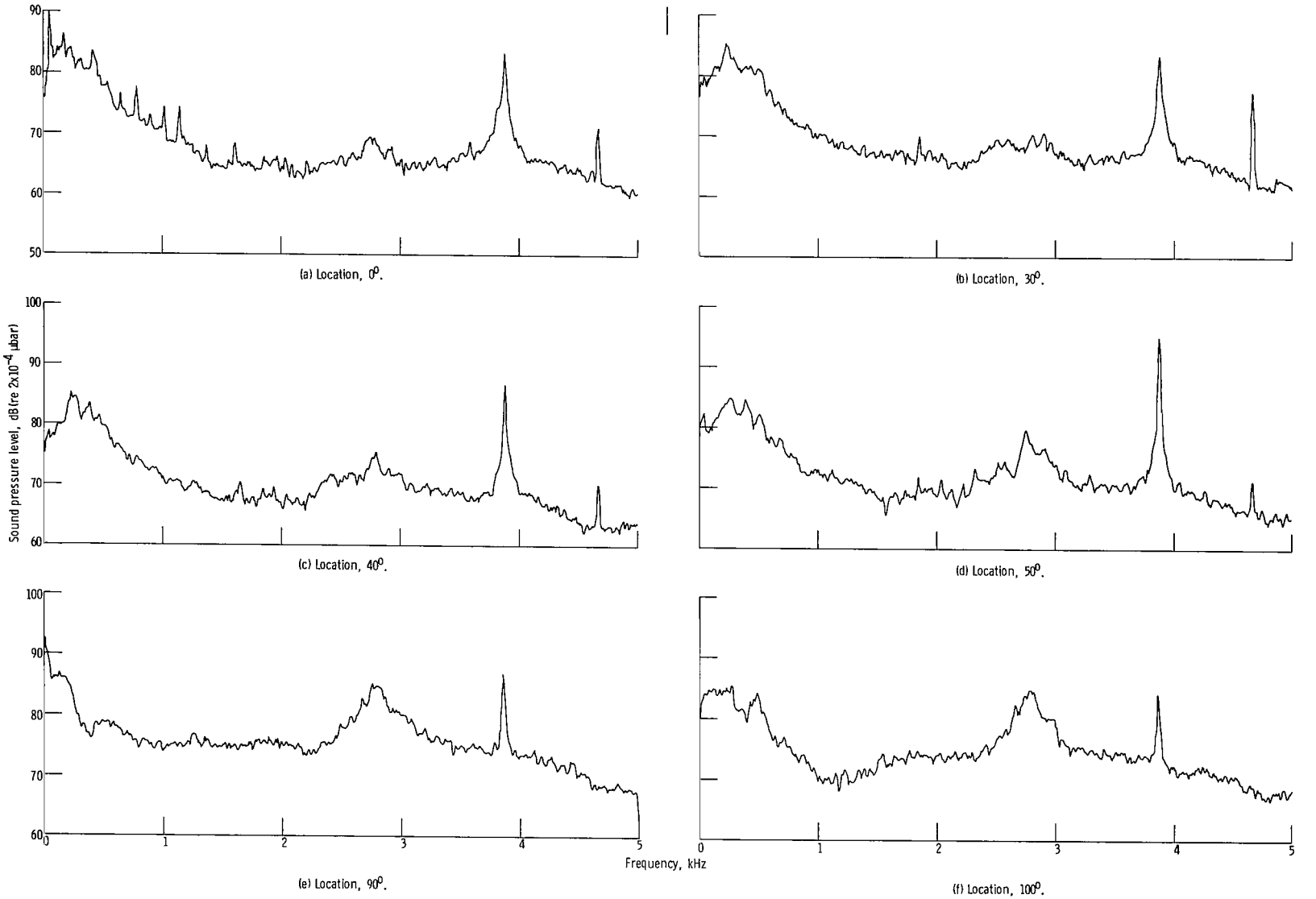

Figure 22. - Engine spectrogram. Nozzle, 0.330 square meter (512 in.^{2}); bandwidth, 16 hertz; bleed rate, 0 percent.

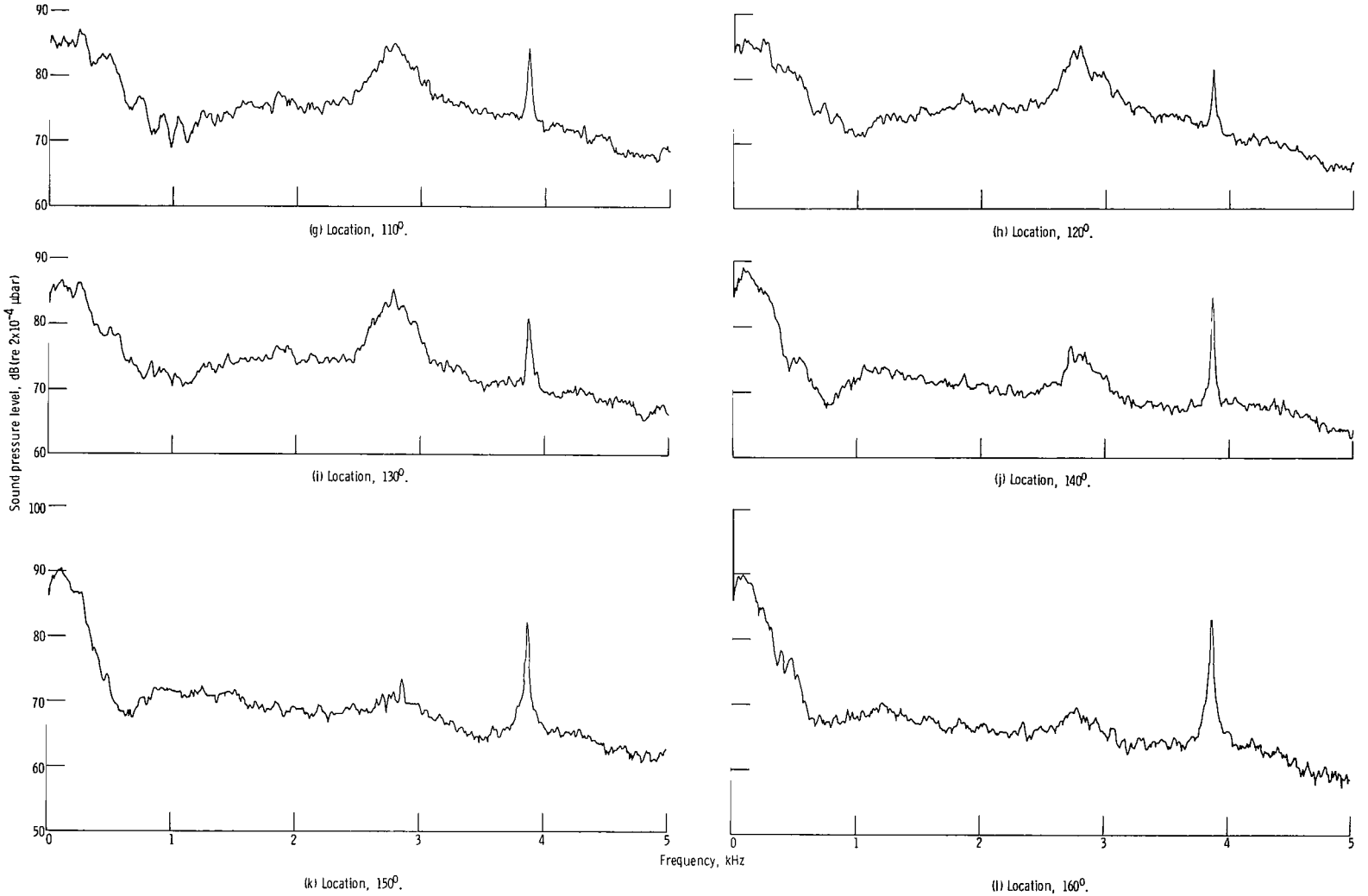

(g) Location, 110°.

(h) Location, 120°.

(i) Location, 130°.

(j) Location, 140°.

(k) Location, 150°.

(l) Location, 160°.

Figure 22. - Concluded.

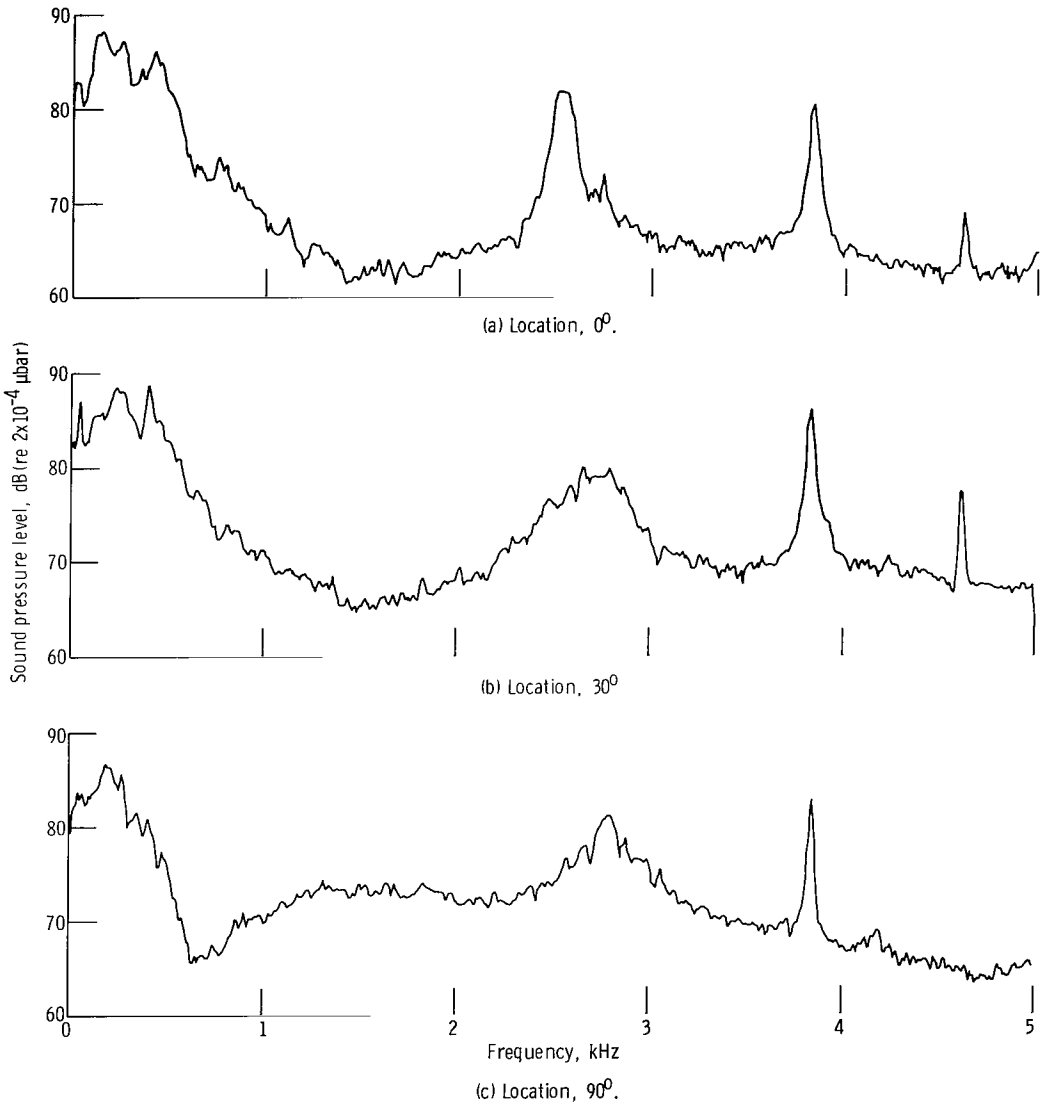

Figure 23. - Engine spectrogram. Nozzle, 0.313 square meter (486 in.^{2}); bandwidth, 16 hertz; bleed rate, 0 percent.

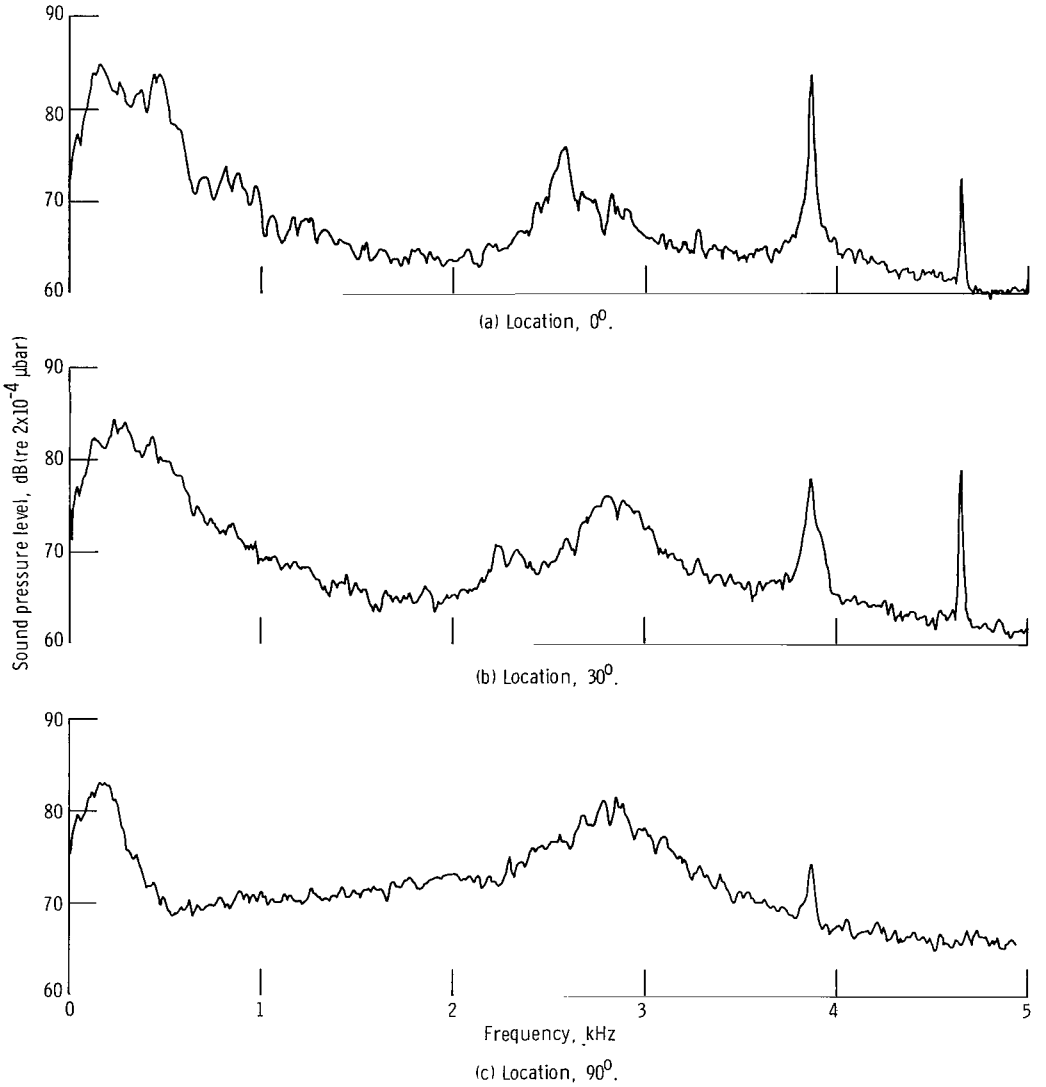

Figure 24. - Engine spectrogram. Nozzle, 0.313 square meter (486 in.^{2}); bandwidth, 16 hertz; bleed rate, 1.2 percent.

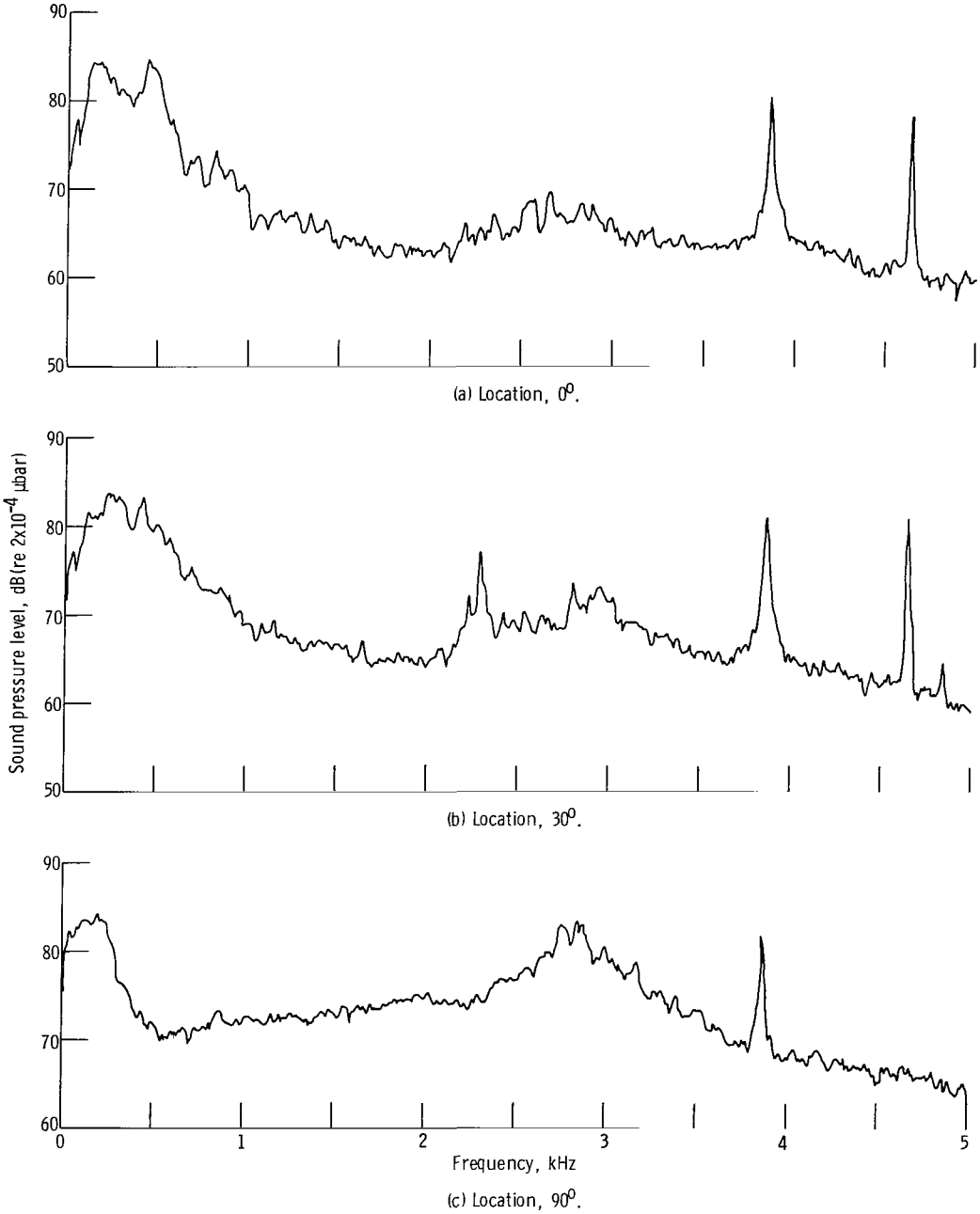

Figure 25. - Engine spectrogram. Nozzle, 0.313 square meter (486 in.^{2}); bandwidth, 16 hertz; bleed rate, 1.4 percent.

NASA-Langley, 1972 —— 1 E-6727

"The aeronautical and space activities of the United States shall be conducted so as to contribute . . . to the expansion of human knowledge of phenomena in the atmosphere and space. The Administration shall provide for the widest practicable and appropriate dissemination of information concerning its activities and the results thereof."

—NATIONAL AERONAUTICS AND SPACE ACT OF 1958

NASA SCIENTIFIC AND TECHNICAL PUBLICATIONS

TECHNICAL REPORTS: Scientific and technical information considered important, complete, and a lasting contribution to existing knowledge.

TECHNICAL NOTES: Information less broad in scope but nevertheless of importance as a contribution to existing knowledge.

TECHNICAL MEMORANDUMS: Information receiving limited distribution because of preliminary data, security classification, or other reasons.

CONTRACTOR REPORTS: Scientific and technical information generated under a NASA contract or grant and considered an important contribution to existing knowledge.

TECHNICAL TRANSLATIONS: Information published in a foreign language considered to merit NASA distribution in English.

SPECIAL PUBLICATIONS: Information derived from or of value to NASA activities. Publications include conference proceedings, monographs, data compilations, handbooks, sourcebooks, and special bibliographies.

TECHNOLOGY UTILIZATION PUBLICATIONS: Information on technology used by NASA that may be of particular interest in commercial and other non-aerospace applications. Publications include Tech Briefs, Technology Utilization Reports and Technology Surveys.

Details on the availability of these publications may be obtained from:

SCIENTIFIC AND TECHNICAL INFORMATION OFFICE

NATIONAL AERONAUTICS AND SPACE ADMINISTRATION

Washington, D.C. 20546